Measurement of Adipose tissue thickness in the body using Medical Ultrasound

By

Gurparkash Singh

AN UNDERGRADUATE THESIS SUBMITTED IN
PARTIAL FULFILLMENT OF THE REQUIREMENTS FOR THE DEGREE OF
BACHELOR OF APPLIED SCIENCE (HONORS)

in the school

of

Engineering Science

SIMON FRASER UNIVERSITY
Spring 2023

Approval

Name: **Gurparkash Singh**

Degree: **Bachelor of Applied Science (Honors) (Biomedical Engineering)**

Thesis Title: **Measurement of Adipose tissue thickness in body using Medical Ultrasound**

Dr. Michael Sjoerdsma, P. Eng
Acting Director, School of Engineering Science

Examining Committee:

Dr. Andrew Rawicz, P. Eng
Professor, School of Engineering Science

Dr. Ash M. Parameswaran, P. Eng
Professor, School of Engineering Science

Dr. Michael Hegedus
Lecturer, School of Engineering Science

Date Approved: **April 17th, 2023**

Abstract

Accurately assessing body composition is crucial in identifying health risks associated with high or low levels of body fat. While there are several methods available for measuring fat, some commonly used methods such as skinfold calipers and bioelectrical impedance analysis (BIA) have limitations and may lead to over or underestimation of fat levels due to factors such as skin elasticity and sweat. In contrast, ultrasound imaging provides a more precise and non-invasive approach for analyzing subcutaneous adipose tissue thickness and identifying the exact separation of muscle and fat. With its portability and ease of use, ultrasound is an excellent assessment tool in situations where other methods may not be feasible. Moreover, it avoids the tissue compression and movement that occur with traditional field methods. The purpose of this study is to describe the technical principles of ultrasound and procedures for measuring and analyzing subcutaneous adipose tissue to determine the fat levels in the body.

Acknowledgements

I would like to express my gratitude to my academic supervisor Dr. Andrew Rawicz for his guidance, motivation, and mentorship throughout this thesis study. Working under him taught me how to step up at challenging times and take charge with confidence.

Further, I would like to thank Dr. Ash M. Parameswaran and Dr. Michael Hegedus for helping me through the writing process and gave freely of their time. Whenever I asked for time, they provided me without restriction.

Next, I would like to mention my thanks to Dr. Ing-Jeng Cheng for educating me with the use of medical ultrasound systems and the marking of measuring sites. This study would not have completed without his contribution.

I would also like to thank my friends and parents for keeping me calm during this stressful period. They provided me with constant support and words of encouragement whenever I needed.

At last, I would like to thank my work employees, my manager, and his family for pushing me forward every single time. The flexibility provided in my work schedule was extremely helpful. Moreover, they helped me reviewing my paper and provided feedback on my work to make it better.

Table of Contents

List of Figures

List of Tables

List of Abbreviations

USI-	Ultrasound Imaging
BIA-	Bioelectric Impedance Analysis
SAT-	Subcutaneous Adipose Tissue
BMI-	Body Mass Index
WHO-	World Health Organization
ISAK-	International Society for the Advancement of Kin anthropometry
DXA-	Dual X-ray Absorptiometry
MRI-	Magnetic Resonance Imaging
CT-	Computed Tomography
RF-	Radio Frequency
TGC-	Time Gain Compensation
SC-	Skinfold Calipers
TEM-	Technical Error of Measurement
B&A-	Bland-Altman
LOA-	Limits of Agreement
PCA-	Principal Component Analysis

Chapter 1. Introduction

1.1. Central Motivation

Obesity is a rising epidemic, as one in three adults in United States are obese. It is widely recognized that obesity is linked to number of health disturbance, such as cardiovascular disease, metabolic abnormalities, hypertension, sleep apnea, and among other [1]. World Health Organization (WHO) defines obesity and overweight as abnormal or accumulation of excessive fat that are associated with body composition and classified by body mass index (BMI). However, BMI does not consider body fat mass or distribution, making it an imperfect parameter for assessing body composition. Assessment of body composition can present a quantitative sign of nutritional status, health, and fitness of individuals. Despite the importance placed on assessing and optimizing body composition, there is no universally accepted measurement method.

Growing consensus over the significance of body composition among the population leads to the advancement in precise quantification of fat tissue compartments. Traditional methods for estimating body fat percentages, such as skinfold calipers, have been used with some success over the years, but the results are variable and may be affected by factors such as skin moisture and metabolic activity. Moreover, these methods require an extensive training to standardize measurements during validation. This highlights the need for more reliable and correct methods for assessing body fat. Ultrasound has been used effectively to assess body fat for nearly five decades, but it remains an underutilized method due to the lack of awareness and standardized protocols [2]. Modern ultrasound devices are now accompanied with software specifically designed for assessing body composition make the results more dependable, reproducible, and accurate. The purpose of this study is to evaluate the reliability and validity of ultrasound technology as a body fat assessment method, and to compare it with traditional methods. The study forms the basis of this thesis.

1.2. Objectives and Contributions

The goal of this research is to evaluate the reliability and validity of ultrasound technology used as body fat assessment method. Objectives for this thesis project include:

- **Objectives:**
  - To compare the adipose tissue thickness measurements from Skinfold Calipers and Ultrasound. This will help to set up the reliability and validity of ultrasound imaging as a method for measuring the subcutaneous adipose tissue thickness.

  - Highlighting Ultrasound Imaging advantages over Surface Anthropometry. This will include the non-invasive nature of using ultrasound as well as capability of obtaining real-time images of adipose tissue that can predict more detailed information about fat distribution and composition.

Successful completion of both objectives will contribute to the current body of knowledge on body composition assessment and may improve the measurement practice in clinical settings and research.

1.3. Thesis Overview

The thesis document has been structured into four different chapters each will investigate into various aspects of the subject.

- **Chapter 1** provides an introduction on the topic and how it became the motivation for continuing with this study. It also mentions the objectives that will be covered throughout this document to fulfil the thesis completion requirements.

- **Chapter 2** supplies a background on the two methods: the skinfold calipers and ultrasound imaging. It also explains why ultrasound imaging was picked as a preferable choice among the two. Moving further, instrumentation for ultrasound has been discussed and described extensively to help making decisions in building ultrasound systems. The chapter ends with talking about two modes of ultrasound which are A-mode and B-mode.

- **Chapter 3** goes forward in the document by providing information on how to mark the measuring sites and collecting the fat thickness using ultrasound. The chapter then explains the required experimentation performed to get the sufficient data for the study to meet the above listed goals. The data collected is further displayed at the end of each experiment.

- **Chapter 4** present the results for the data collected in chapter 2 by performing various statistical analysis to help making the correlation between both methods. These methods include box plot comparison, Bland-Altmann chart, and linear regression model to understand how closely both datasets are to each other and whether it is applicable to replace one method with another. The study helps answering the question, which method is better and on what basis. The discussion part of this chapter talks about the results whether they can fulfil the required objectives or not. The discussion will also describe the challenges that were faced during the study and limitations of both the methods.

- **Chapter 5** concludes the thesis with a summary about the fulfilment of the objectives and a brief discussion about the potential future work.

Chapter 2. Background and Instrumentation

2.1. Background: Skinfold calipers

Skinfold thickness illustrates the amount of subcutaneous fat when the fold is lifted, and its thickness measured by specialized calipers. These specialized calipers are prescribed by International Society for the Advancement of Kin anthropometry (ISAK), and they take about 30 minutes for full profiling of the body [3]. The callipers are readily available and easily calibrated since the ISAK requires use of callipers that are regularly calibrated. Skinfold callipers require a constant closing compression of 10 g/mm^2 and should be calibrated to at least 40 mm in 0.2 mm divisions.

The advantage of skinfold calipers is that it is small, uncomplicated, and a quick measuring procedure to record the accumulation of subcutaneous fat. Although the subcutaneous adipose tissue (SAT) measurement using skinfolds has a long tradition, the accuracy obtained using this technique is limited [4]. In this method, skin and SAT are measured together in a compressed state without considering the compressibility and viscous-elastic behaviour at the individual measurement sites. Moreover, the measurements may slightly differ from one another due to the location of skinfold and grasping techniques at those sites [5]. Therefore, to drop potential discrepancies, a novel ultrasound technique using standard B-mode (brightness mode) ultrasound machine has been introduced to measure the thickness of SAT.

2.2. Background: Ultrasound

Ultrasounds are classified as sounds that have frequencies higher than the highest frequency a person can hear. This says that any sound above 20kHz is ultrasound. However, for medical purposes, the ultrasound systems typically work between 1-10MHz with an addition of a few specialized systems operating in ranges up to 70MHz. Its use in medical imaging applications goes back to mid-1950s but the expansion began in the early 1970s due to the arrival of two-dimensional real-time ultrasonic sensors [6]. Since then, new milestones were achieved every decade in the form of passed array systems, color flow-imaging systems, three-dimensional systems, and nonlinear imaging systems.

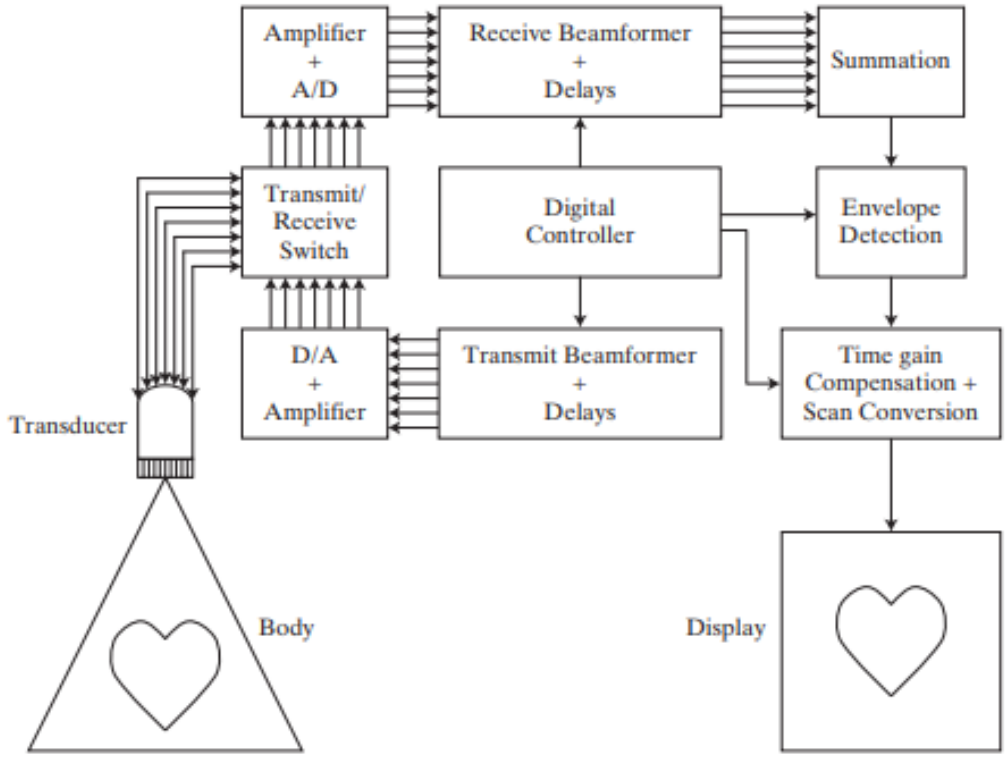

Fig.1. Block Diagram of an Ultrasound System [6]

An ultrasound transducer made up of piezoelectric crystals that converts electrical signals into acoustic signals, generating a pulse of ultrasound that is transmitted through a person's body. When the beam of pulses encounters organ boundaries or complex tissues, they produce echoes that return to and are detected by the transducer. The echoes are converted into electrical signals and are processed by ultrasound imaging system to present a grayscale image of echo-generating structure of the body. A block diagram for an ultrasound imaging system is shown in Fig.1.

Most ultrasound systems used in medical field use the same transducer for both generation and reception of the sound waves as displayed in the diagram in Fig.1. This is known as pulse-echo mode of operation. The transducer is coupled to the skin using an acoustic gel, and then a brief pulse like acoustic wave is generated. The wave then propagates into the body, where a part of it reflects and detected by the transducer [6]. The transducer then converts acoustic wave sensed at its face to an electrical signal which is amplified, stored, and displayed as an image on the screen.

The fundamental principle of ultrasound imaging is based on the reflection and scattering of ultrasound by the body tissues in the path of the beam. The amount of sound reflected is dependent upon the change in acoustic pressure which further depends on change in acoustic (characteristic) impedance between two tissue surfaces [2]. Acoustic impedance (Z) is defined as the product of tissue density with speed of sound (acoustic velocity) and is given by:

$$Z = \rho c \tag{1}$$

where ρ and c are the tissue density and acoustic velocity, respectively. Table I below, display the acoustic properties for varied materials.

TABLE I
ACOUSTIC PROPERTIES OF VARIOUS MATERIALS [6]

Material	Density, ρ [kg m^{-3}]	Speed, c [m s^{-1}]	Characteristic Impedance, Z [kg m^{-2} s^{-1}] ($\times 10^6$)
Air at STP	1.2	330	0.0004
Aluminum	2,700	6,400	17
Brass	8,500	4,490	38
Castor oil	950	1,500	1.4
Mercury	13,600	1,450	20
Polyethylene	920	2,000	1.8
Polymethyl-methacrylate	1,190	2,680	3.2
Water	1,000	1,480	1.5
Blood	1,060	1,570	1.62
Bone	1,380–1,810	4,080	3.75–7.38
Brain	1,030		1.55–1.66
Fat	920	1,450	1.35
Kidney	1,040	1,560	1.62
Liver	1,060	1,570	1.64–1.68
Lung	400		0.26
Muscle	1,070		1.65–1.74
Spleen	1,060		1.65–1.67
Water	1,000	1,484	1.52

As mentioned in Table I, air has almost no impedance, while fat and muscle have impedances closer to each other, and bone has a relatively high acoustic impedance. Therefore, echoes reflected from muscle-fat interface will be weaker as compared to muscle-bone interface or muscle-fat interface. The relative strength of the echoes is represented by the brightness of generated grayscale image [6]. As mentioned above, anything above 20kHz is ultrasound, so as the frequency increases, the resolution also increases but at the cost of reduce depth of

penetration as it is inversely proportional to the frequency used. The formula for depth (D)of penetration is given by:

$$D = \frac{L}{2af} \tag{2}$$

where L is the dB loss of signal (typically 80dB), f is the frequency and, a is the intensity reflection coefficient which is calculate using the absorption coefficients of two penetrating media.

Generally, the frequency of ultrasound is kept around 5-7MHz, but it is changed depending upon the measuring sites. For fat measurement, the speed of ultrasound used is 1450m/s (from Table 1) and further this will be used to calculate the distance between probe and the tissue [7]. The Fig.2. shows the difference between reflected brightness areas depending upon the tissue and their interfaces.

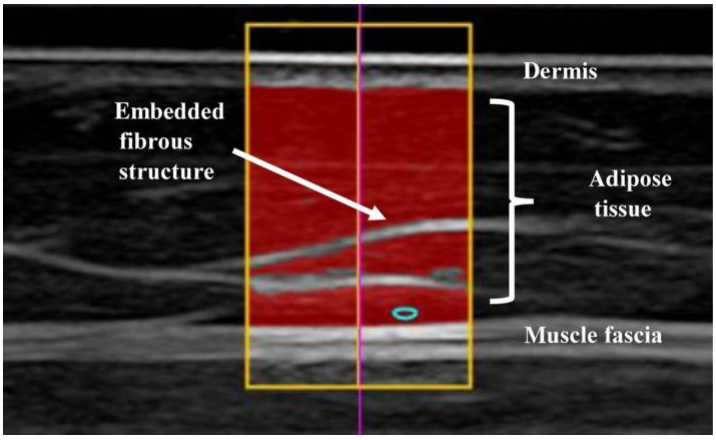

Fig. 2. Ultrasound Image at the front thigh with highlighted fat area [7]

The shortest distance i.e., the perpendicular distance between the upper edge of the dermal/adipose interface and the upper edge of the adipose/muscular interface will provide us the subcutaneous adipose tissue as shown in Fig.2. The accuracy of fat measurements primarily depends on the image resolution as it ranges from 0.1mm (18MHz linear transducer) to 0.3mm at 6MHz. However, in obese individuals, where subcutaneous fat is several centimetres thick, the resolution can be neglected as most area in the scan will be pitch dark and bright borders will appear clearer and more separated. Therefore, it is not a main concern whether to detect borders with resolution of 0.1mm or 0.3mm as it will not reduce the accuracy considerably, provided that the speed of sound is set correctly [8].

2.3. Motivation: Ultrasound

Measurement of body composition is a crucial aspect of assessing overall health and fitness. While various methods are available to assess body composition, including air displacement plethysmography, bioelectrical impedance analysis, and skinfold measurements, they all have limitations in terms of time, equipment, and accuracy [9]. Although surface anthropometry is an easy and well-tested method, it requires an extensive practice to generate some practical results. Moreover, the use of calipers is limited by their range (approximately 60 mm), which can cover only a part of the clinical population. [10].

There are various techniques available to measure body composition, such as Magnetic Resonance Imaging (MRI), dual X-ray absorptiometry (DXA), and Computed Tomography (CT scan). However, these methods involve exposure to radiation and are not possible for daily use due to their excessive cost and poor cost-to-clinical-benefit ratio. Although MRI is considered the gold standard for calculating body fat content and distribution, its excessive cost and limited availability restrict its use in routine clinical practice [11]. On the other hand, ultrasound technology for body composition assessment has been gaining popularity in recent years due to its portability, clear-resolution imaging, and potential for use in clinical settings. The use of ultrasound technology can provide accurate and reliable results, even in field-based settings, which makes it a promising choice for body composition assessment. It has the capability of not just producing the whole-body assessment but also site-specific evaluation and faster than other laboratory methods [2]. With its widespread availability and its use in clinical environments, ultrasound technology has the potential to become a more practical and feasible way for routine body composition assessment.

2.4. Ultrasound: Instrumentation

Ultrasound instrumentation consists of a complex interplay of electronic components, mechanical systems, and software that work together to perform medical diagnosis. Although building an ultrasound sensor specifically for measuring fat thickness is relatively straightforward, the construction and calibration of the various components must be done with care to ensure accurate and reliable results. The core components of an ultrasound machine include a transducer, pulser-receiver, beamformer, signal processor, and display [12].

2.4.1 Piezo-electric Effect

There are many ways by which acoustic waves can be generated. In fact, any change in the pressure field or the stresses within the medium will induce such waves. The most common method of generating ultrasound, and the one employed in the devices used in clinical ultrasound, relies on a phenomenon called the piezoelectric effect as it enable us to control the transmitted signal on one hand and is also sensitive enough to detect waves or echoes on the other hand [13]. Piezoelectric materials have been used for many decades and their variety and new uses are steadily growing.

The piezoelectric effect is a phenomenon where certain materials, known as piezoelectric materials, can convert mechanical energy into electrical energy. The word "piezo" comes from the Greek word for pressure [13]. When piezoelectric materials are subjected to mechanical stress, such as compression or stretching, electrical charge accumulates on their surfaces, resulting in an electric potential difference. This effect is useful in detection of ultrasonic waves. Fig.3. illustrates this effect and shows the polarity of the induced surface charges.

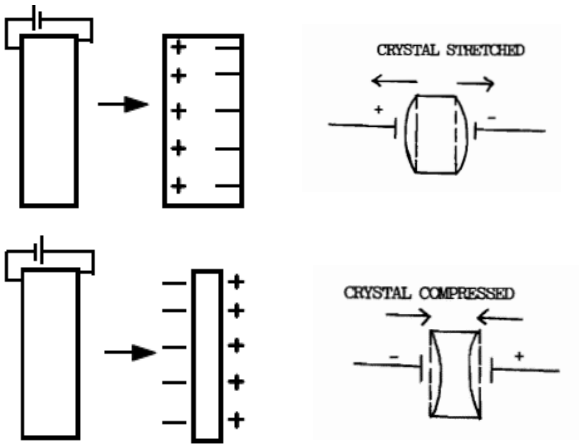

Fig. 3. Describes the Piezoelectric phenomenon with the change of polarities. [14] [13]

However, when a potential difference is applied between the faces of a piezoelectric crystal, the crystal will respond by expanding or contracting. Electrical energy will have been converted to mechanical energy and this is known as reverse piezoelectric effect. This effect is used in in the production of ultrasound waves.

When a piezoelectric crystal is subjected to a high-frequency alternating voltage, it will vibrate (20000 times per second) and produce ultrasound waves [14]. The frequency of the ultrasound is found by the applied voltage and the physical properties of the crystal. If voltage is applied for an extremely brief time, then the crystal resonates at its own frequency and a pulse is produced. Truly short pulses are used for producing the ultrasound diagnostic images. In summary, production of ultrasound relies on the reverse piezoelectric effect, while detection is based on the piezoelectric effect. Because of the reversibility of this phenomenon, it is possible to use the same crystal to produce ultrasound, and later to detect echoes returning to the crystal from a reflector at some distance away.

2.4.2 Transducers

The transducer is a crucial component in ultrasound technology, responsible for generating and detecting ultrasound waves. It consists of an array of piezoelectric elements with electrodes on opposite sides of it that can be activated simultaneously to produce an ultrasound pulse by converting electrical energy to acoustical energy and vice versa [15]. The electrodes are made by plating a thin film of gold or silver on the crystal surface. The transducer consists of backing behind the element that controls the amplitude of oscillations [16]. The backing material decides the bandwidth of the transducers. The Fig.4. label all the other elements of a single-element transducer.

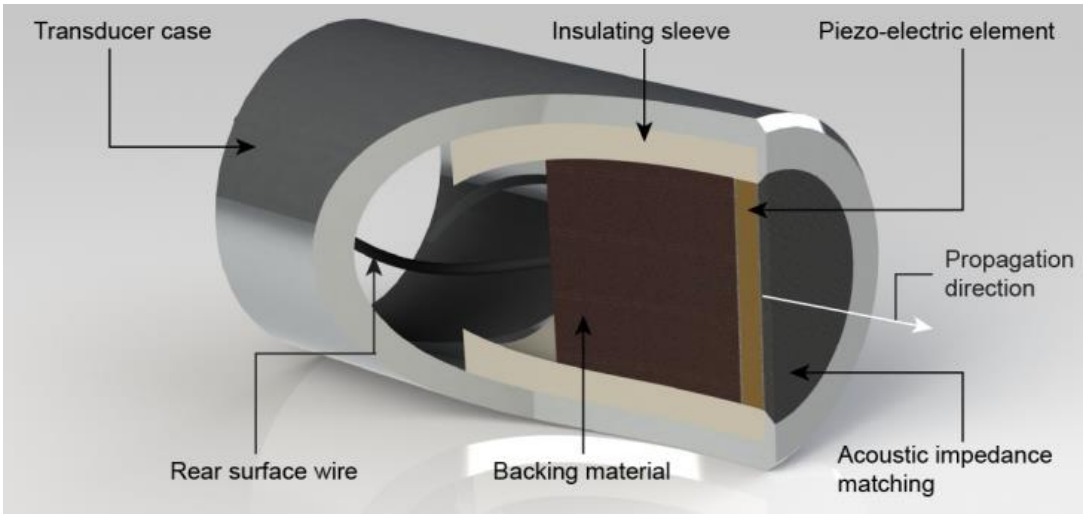

Fig. 4. Components of a single-element transducer [16]

However, the transducer is sensitive to electromagnetic interference, which can contribute to a higher noise level that does not correspond to physical interactions of sound waves with the tissue. To reduce this interference, a radiofrequency shield composed of a hollow metallic cylinder is placed around the crystal [12]. This shield acts as a Faraday cage, preventing external electromagnetic waves from entering the transducer and affecting its performance.

The entire assembly housed in an electrically insulating casing, that not only provides structural support but also further minimizes the risk of electromagnetic interference. The casing is usually made of plastic or rubber, materials that are not conductive and do not interfere with the piezoelectric elements' performance.

There are several unique designs of the transducer depending on the usage and number of piezoelectric crystals used [13]. However, since the study requires to measure the SAT thickness, a single crystal transducer is sufficient to do the job. This way, it will be cheaper than the other ultrasonic sensors available in market and can be labeled as a household medical device too.

2.4.2.1. Dynamic Damping and Pulsed-Wave Output

Dynamic damping is an electronic method used to suppress resonance, also known as ringing, which occurs in the piezoelectric crystal. When an excitation pulse is applied to the crystal, it can cause the crystal to vibrate at its natural frequency, which can result in unwanted ringing that can interfere with the accuracy of the ultrasound signal. To prevent this, a voltage of opposite polarity is applied via damping block (usually tungsten/rubber in epoxy resin) to the crystal instantly following the excitation pulse [12]. This counteracts the expansion and contraction of the crystal that is stimulated by the first pulse, effectively damping out the oscillations.

2.4.2.2. Pulse Repetition Frequency

The number of times the crystal is pulsed or electrically stimulated per second is called the pulse repetition frequency. Since transducer cannot send and receive ultrasound at the same time, a limit exists with respect to the rate at which it can be pulsed. The maximum pulse repletion frequency (PRF_m) is limited by the maximum depth (R) to be sampled and the velocity of ultrasound (c). The equation is given by:

$$PRF_m = \frac{c}{2R} \tag{3}$$

The factor of 2 accounts for the distance down to the interface and back to the transducer. The equation above illustrates that PRF_m can be increased by increasing the velocity of sound in medium or by decreasing the depth of interest [12]. Typically, velocity stays the same in the medium, so depth is the only potential parameter capable of being changed. However, the systems have the capability to vary PRF with the depth, so the operator doesn't have to change this manually.

2.4.2.3. Ultrasonic Field

The shape of the ultrasound field plays a crucial role in obtaining high-quality results. It's essential for the field to be directional instead of non-directional. If a point source is used, the waves are emitted in all directions, resulting in poor resolution. On the other hand, a large-diameter transducer produces a unidirectional beam with planar wavefronts, and the lateral extent of the beam is nearly the same as the diameter of the crystal [12]. However, if the diameter of the sound source is increased to several wavelengths, each small area will function as an individual vibrating sound source producing its own spherical wavefronts. These waveforms undergo constructive and destructive interference, leading to a very complex wave pattern as illustrated in Fig.5. This complexity can degrade the quality of the ultrasound image, so it's important to carefully design the transducer to generate the desired ultrasound field.

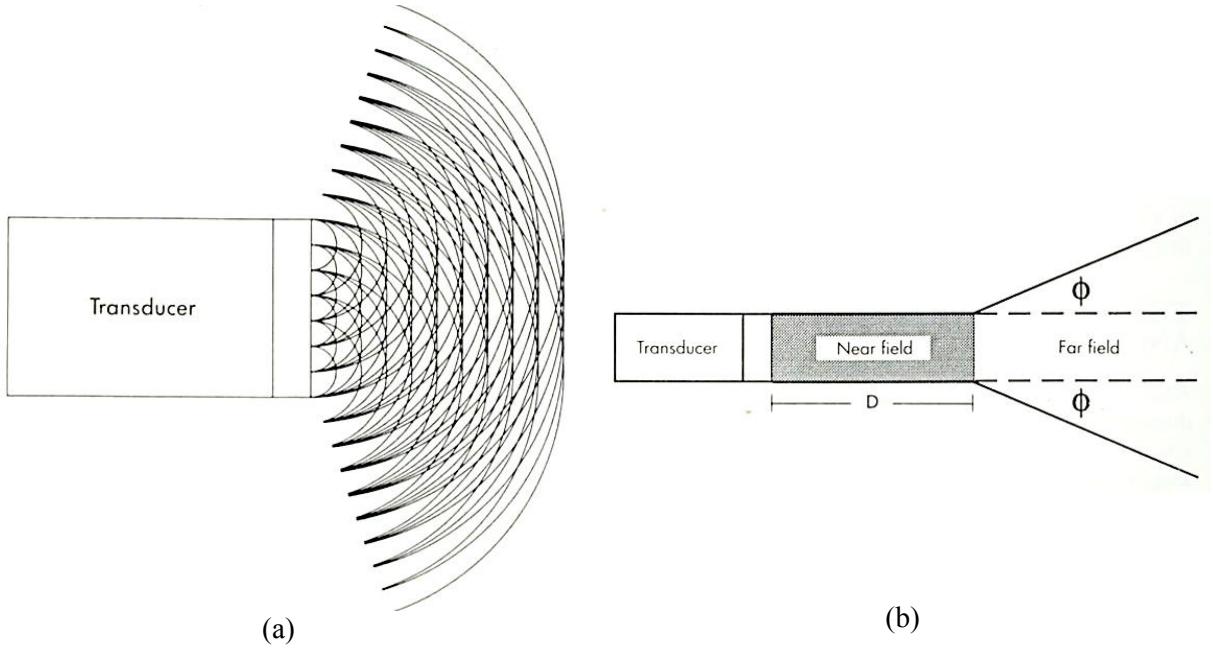

(a) (b)

Fig. 5. (a) Large sound source acting as multiple sources. (b) Beam pattern showing the near field and far field. D indicates the depth of near field [12]

The Fig.5. shows a non-uniform beam intensity in the near field and a uniform beam in the far field, where the lateral resolution is poor. Lateral resolution refers to the ability to detect small objects across the width of the beam. In the near field, the width of the beam is preserved, and therefore, a uniform beam is desirable to achieve best results.

2.4.2.4. Transducer Selection

Selecting the type of transducer depends on the depth of interest. The goal is to improve the lateral resolution by scanning the area with a narrow beam. Large-diameter transducers have a wide near-field beam, resulting in poor lateral resolution at shallow depths. In contrast, the near field extends to greater depths in the body with a smaller diameter transducer [12]. The beam divergence in the far field is also less for larger transducers as shown in Fig.6., making them preferable for imaging deep-lying structures.

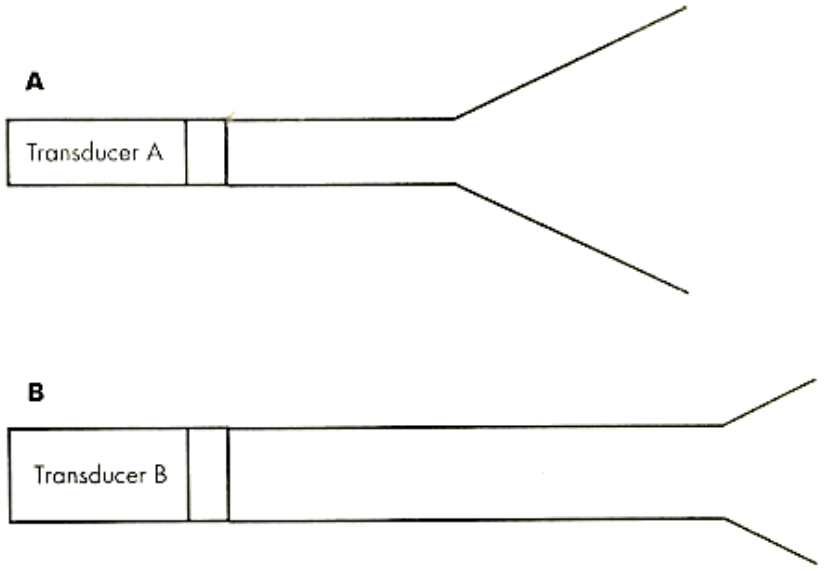

Fig. 6. (A) smaller-diameter transducer can maintain a narrow beam width. (B) Larger diameter transducer with larger beam width and better lateral resolution [12]

A similar effect is observed with frequency, with all other factors constant, an increased frequency results in a deeper near field and a less diverging far field. Therefore, if shallow structures and irregular surfaces are of interest, a small-diameter high-frequency transducer should be used [12].

2.4.3 Transmit Gain

In ultrasound imaging, attenuation can affect image quality by making the target appear too bright or too dark. To address this, the power can be adjusted either throughout the entire image or at specific depths [17]. Most ultrasound machines have an output, power, or transmit gain control that adjusts the voltage spike to the transducer, resulting in an acoustic pulse of higher intensity. This results in a stronger echo as shown in Fig.7. below.

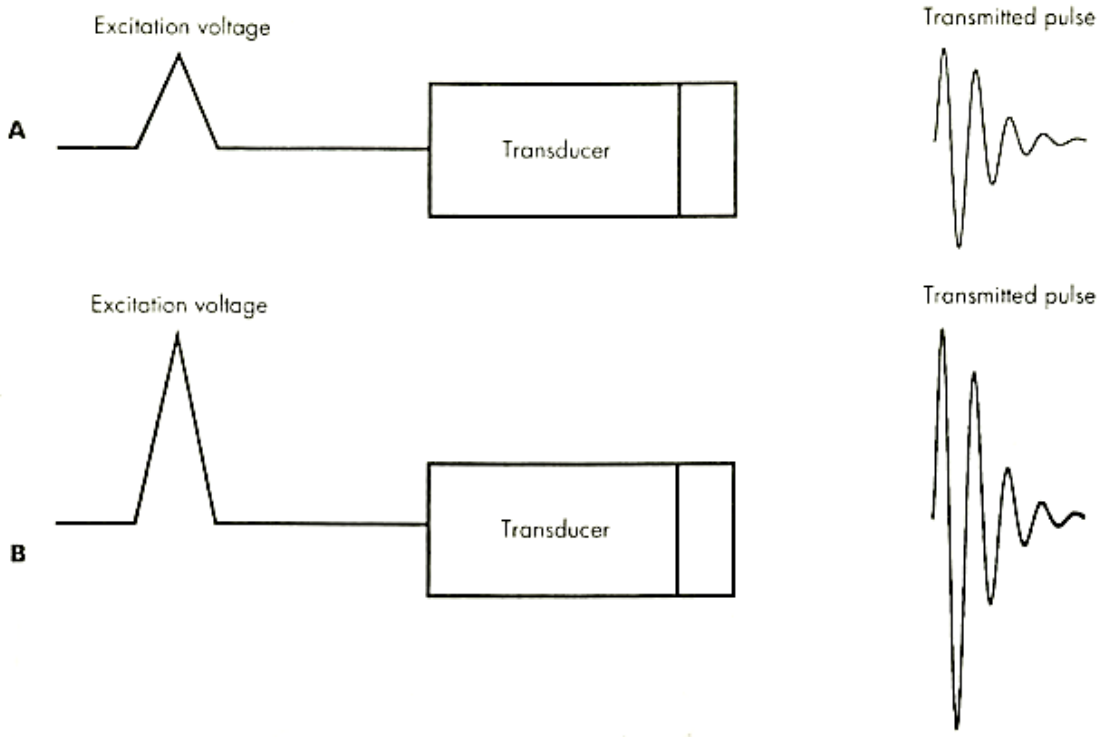

Fig. 7. Excitation voltage regulates the transmitted beam intensity.
(A) Low voltage (B) High voltage [12]

The typical excitation voltage pulse ranges from 300-600V but can be as high as 900V, and this control is available on the control panel of the ultrasound system or in the software [12]. The transmit gain control is adjustable in 3dB increments.

2.4.4 Amplification

When the ultrasound wave strikes the crystal, it causes the crystal to vibrate and generate an echo in the form of waves. This vibration induces a radiofrequency signal via the piezoelectric effect. The resulting RF signal waveform mimics the ultrasound waveform since the voltage variations are in response to pressure-induced thickness changes in the crystal [12]. This is represented in the form of waveforms in Fig.8. The RF signal, typically in the microvolt or millivolt range, is amplified to a level between 1V to 10V which helps in processing and displaying the results. The receiver gain amplification used is commonly logarithmic, which allows for weak signals to be amplified more than strong signals. This is important for enhancing the overall image quality and minimizing noise [12]. The receiver gain is usually adjustable by the operator to optimize the amplification for the specific imaging task at hand.

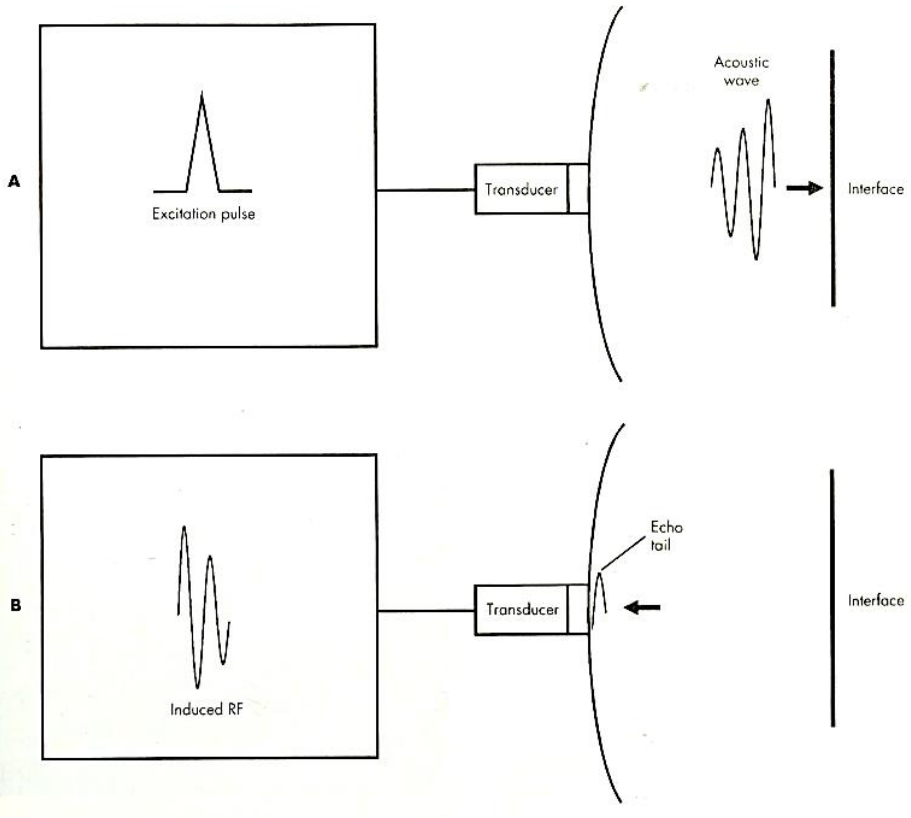

Fig. 8. Transmission and reception of signals. (A) Acoustic wave initiated by the excitation pulse applied to the transducer. (B) The echo on return to the transducer induces the radiofrequency signal. [12]

2.4.5 Time Gain Compensation

Time gain compensation (TGC) is a technique used to adjust the power of ultrasound signals at specific depths to combat attenuation. This is particularly useful for improving the imaging of deep structures, especially in cases where posterior acoustic enhancement occurs [17]. By equalizing the signal strengths or brightness levels of reflectors with equivalent size, shape, and reflection coefficient, it becomes easier to show and analyze them. TGC controls are typically adjustable by the operator and can help produce clearer and more correct ultrasound images.

In addition to compensating for attenuation, TGC can also contribute to signal compression. When scanning the liver, for example, all echoes should be of nearly the same amplitude, unless an abnormality is present. This feature is often seen with "slider bars" on the ultrasound console, although automatic TGC can adjust varying gain without operator intervention [12]. The amount of amplification is decided by the general decrease in echo-induced signal amplitude.

2.4.6 Signal Processing

The RF signal induced in the transducer by returning echoes undergoes several processing steps before it is displayed. After amplification and TGC, the signal is rectified to drop its negative part [18]. Any signals below a certain threshold are electronically rejected, and the remaining signals are enveloped to produce a processed signal that can be further amplified for display purposes [12]. These accepted signals are organized based on their anatomical location and intensity, and different display modes such as amplitude mode (A-mode) or brightness mode (B-mode) can be used to visualize the information.

2.4.7 A-mode Scanning

The envelope detected signal is the foundation of ultrasound systems, which is also known as the A-mode signal or amplitude-mode signal. This mode displays the returning echo signals as spikes, which are plotted along a time scale as shown in Fig.9. The amplitude of the signal is displayed on one axis, while the position of the signal is represented on the other axis (horizontal). Only structures that lie along the direction of propagation are interrogated.

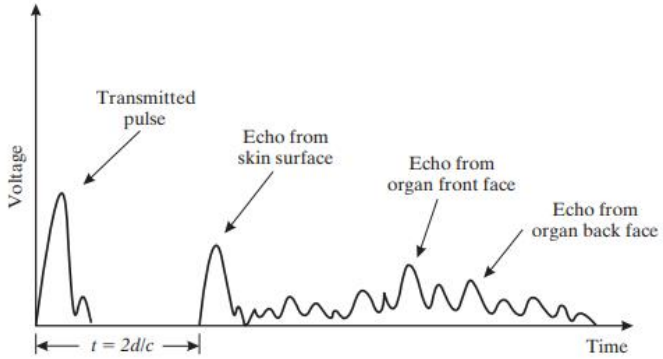

Fig. 9. A typically A-mode display *[6]*

The time axis in the A-mode scan represents the time delay between the ultrasound pulse and the returning echo [12]. This time delay is proportional to the distance between interfaces. By converting the time axis to depth information, the A-mode scan also holds spatial information by registering the distances between interfaces. Multiple interfaces encountered along the sampling direction are detected by the series of echoes shown in Fig.9. The three interfaces shown are from skin, organ front face, and back face respectively [6].

A-mode information is valuable for tissue characterization as the detected echoes can be displayed in an unaltered form. This can be used as a valuable and an inexpensive tool to measure the fat thickness. The Fig.10. below shows an A-mode graph for an abdominal scan. The yellow shaded area below stands for the subcutaneous fat, in this case about 9.5mm [2].

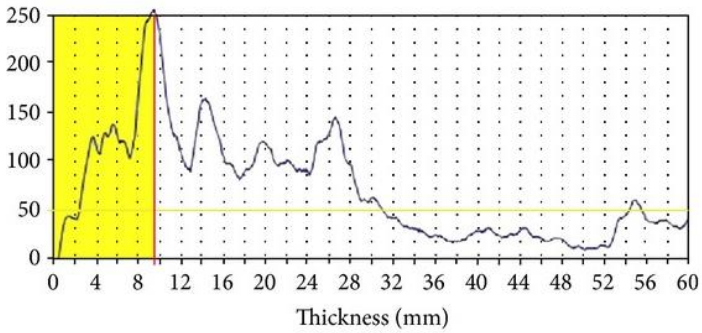

Fig. 10. A-mode Scan for Abdomen *[2]*

A greater dynamic range of signals is preserved in A-mode scan as compared to other imaging techniques. Identification of cysts in the breast is occasionally done by A-mode scanning [12]. Fig.11. shows the block diagram for A-mode scanner with all the components labeled.

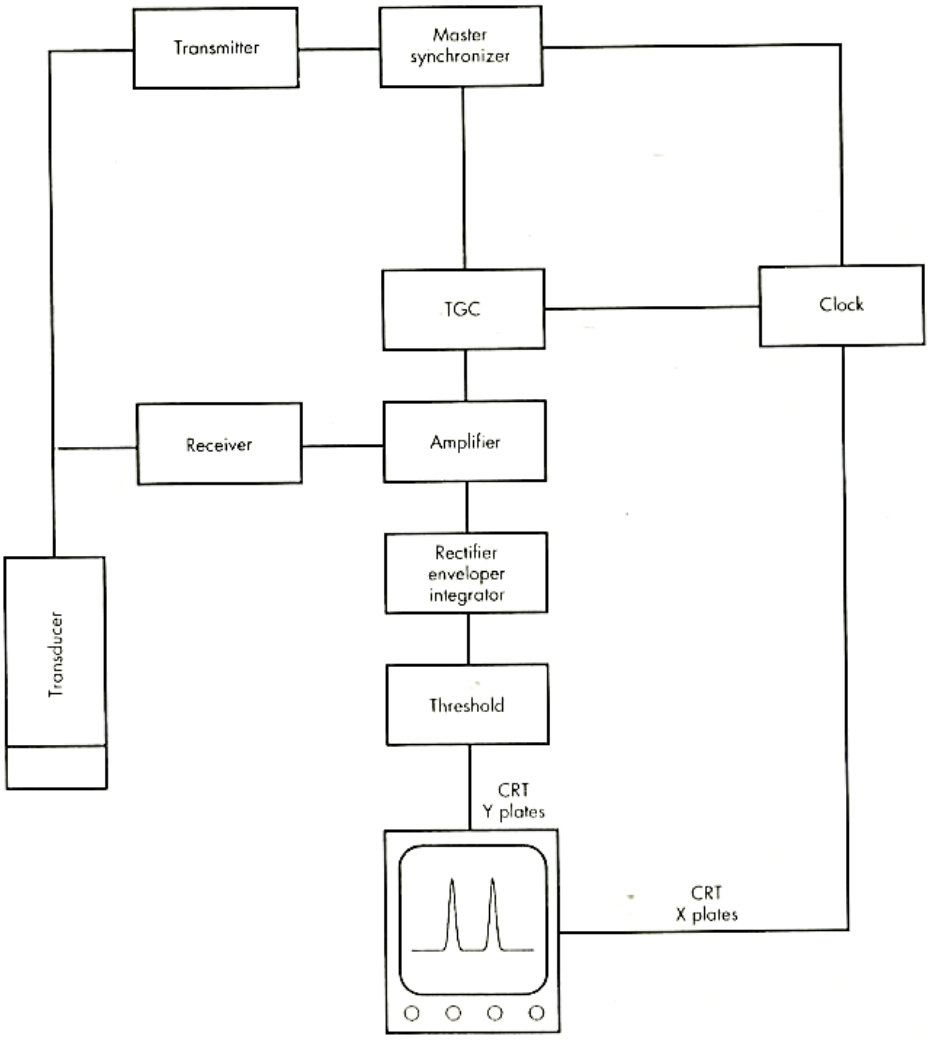

Fig. 11. Block diagram for A-mode scanner [12]

The master synchronizer initiates the scanning process by sending the voltage pulse to the transducer via transmitter. The excitation of crystal inside transducer generates a pulsed ultrasound wave that directed into the body. The clock, activated by the master synchronizer measures the elapsed time from the transmission that is used to measure the depth of the interface based on the constant velocity of ultrasound in tissue [12]. At last, the results are displayed on the display in the form of peaks. The height of those peaks indicates the strength of received echoes while the position along horizontal denotes the depth of interfaces.

2.4.8 B-mode Scanning

In brightness mode, signals from returning echoes are displayed as dots of varying intensities. The spike of the A-mode is replaced by a small dot which can be shown by rotating the spike 90 degrees out of the plane of the paper [12]. The intensity of a dot (the brightness) is a relative measure of the echo size, with large echoes appearing as very bright dots, while non-reflectors appear as dark dots. The position of the dot represents the depth (time) of the interface from the transducer. Fig.12. shows a comparison of A-mode and B-mode signals. The points for B-mode scan are plotted on an intensity (y-axis) v/s depth (x-axis), while A-mode signals are plotted on amplitude v/s time or depth depending on the requirement.

Normally, most ultrasound diagnostics are interested in constructing a 2-D image for the area of interest rather than getting data from a single scan line. This is conducted by compound B-scanning where multiple sets of dots are combined to form the internal structures within the body. In a way, each column of B-mode can be considered as a form of A-mode data [15].

In the early days of ultrasound, the transducer had to be swept across the area of interest and scans were taken from various directions. The superposition of these scans resulted in a static 2-D image [12]. However, modern advancements in transducer technology have ended the need to take multiple scans. Instead, images are generated with the transducer probe held in one position. The most common type of scanner used today is the linear array, which comprises a collection of transducers arranged in a straight line, mimicking the linear translation of a single transducer without requiring motion [6].

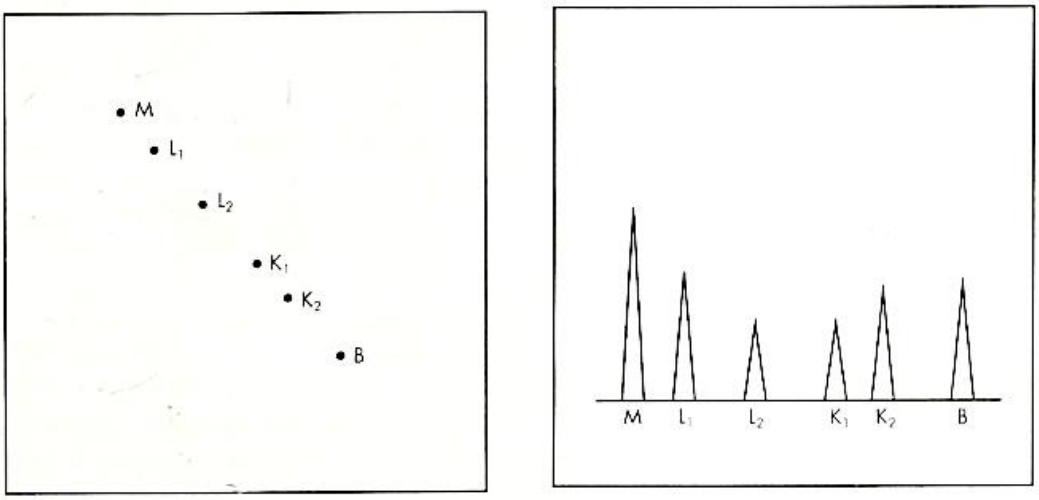

Fig. 12. Comparison Between B-mode (left) and A-mode (right) display. [12]

The block diagram in Fig.13. shows how the above listed components of ultrasound can be integrated together to form a small handheld device.

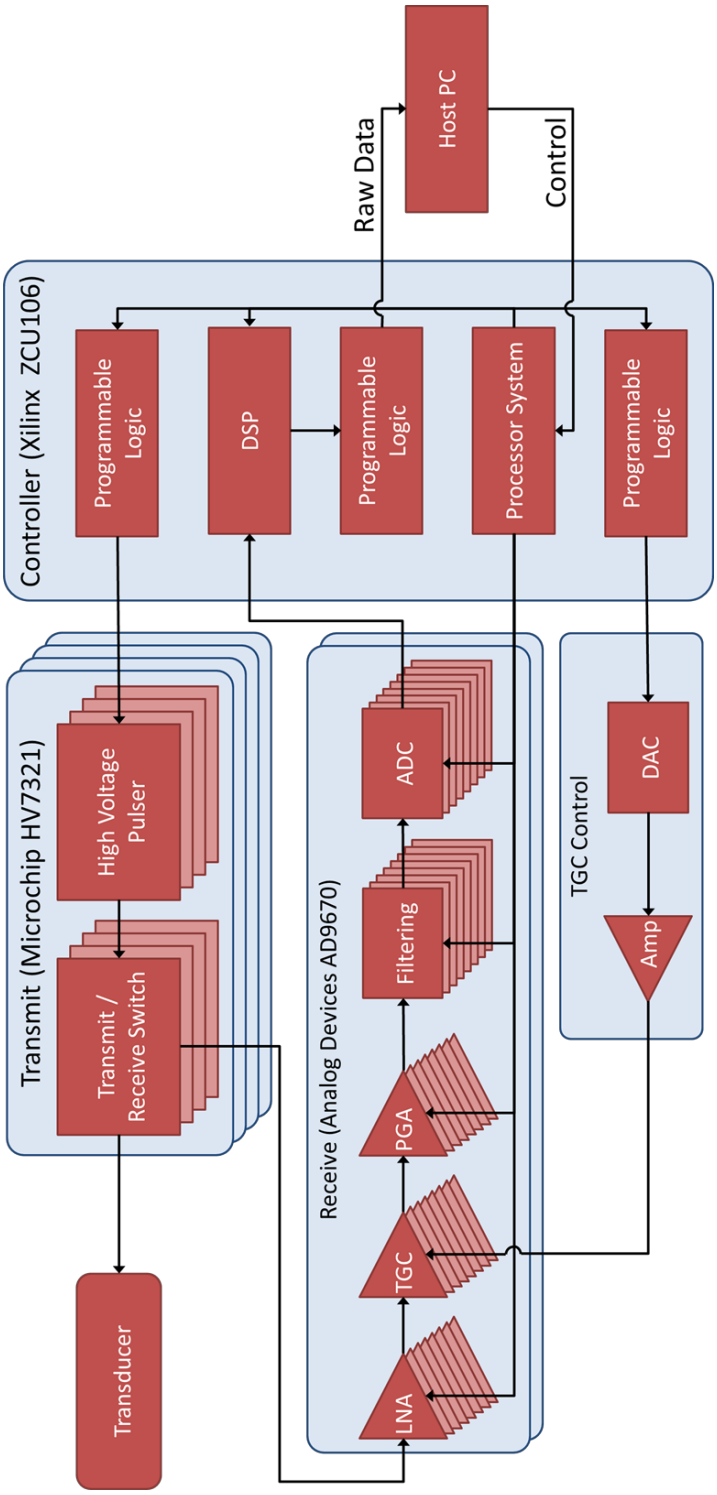

Fig. 13. Block diagram for an Ultrasound Prototype [26]

Chapter 3. Experimentation

3.1. Data Collection Procedure

Considering the entire body, ultrasound subcutaneous fat thickness evaluation technique comprising of eight standardized sites comprising: upper and lower abdomen, erector spinae, distal triceps, brachioradialis, front thigh, medial calf, and lateral thigh has been proposed to maximize both accuracy and reliability [19]. Table II describes how to mark the standardized sites and take the ultrasound images at each of them [8].

TABLE II
DESCRIPTION OF ULTRASOUND SITES AND MEASUREMENT PROCEDURE

Site Name	Description of the sites	Notes on US image capture
Upper abdomen (UA)	1. Mark a vertical line at a distance d=0.02 h (i.e., 2% of body height h) lateral to the centre of the umbilicus. 2. Project vertically and mark a horizontal line at d=0.02 h superior to the Omphalion.	Lying in a supine position Participant must stop breathing at mid-tidal expiration and then the image is captured
Lower abdomen (LA)	1. Same (1) as for the upper abdomen 2. Project vertically and mark a horizontal line at d=0.02 h inferior to the omphalion. Measure always exactly at this point	Same as upper abdomen
Erector spinae (ES)	1. Mark a transverse line at d=0.14 h above the solid surface while sitting in a stretched upper body position with thighs horizontal and legs unsupported 2. Mark the site at d=0.02 h lateral to the spinous process of the vertebra	Lying in a prone position

Distal triceps (DT)	1. Put the lower arm on a table with the hand in the mid-prone position; mark a vertical line on the most posterior aspect of the arm. 2. Mark the site on the vertical line at a distance from the surface of d=0.05 h	Lying in a prone position. Capture the image with the dorsal surface of the hand on the table. Make sure the probe orientation is perpendicular to the skin
Brachioradialis (BR)	1. Place the forearm with the hand in the mid-prone ('shake-hands') position on a support table and contracts the brachioradialis. 2. Draw a longitudinal line on the most anterior surface of the brachioradialis muscle. 3. Mark a transverse line at a distance d=0.02 h distally from the anterior surface of the biceps brachii tendon. Project this line transversely to intersect with the longitudinal line	Lying in a supine position Take the image with the arm in a mid-prone position and in contact with the thigh. Avoid imaging the vein in case there is one in the vicinity.
Front thigh (FT)	1. Put the foot on the anthropometric box placed in front of a wall such that the thigh is horizontal, and the big toe and the knee touch the wall. 2. Mark the site at a horizontal distance d=0.14 h from the wall.	Lying in a supine position.
Medial calf (MC)	1. Place the foot on the anthropometric box such that the thigh is horizontal and the leg vertical. 2. Mark the site at d=0.18 h above the surface at the most medial aspect	Lying in a rotated position Participant rolls onto the right side with the right knee at a 90° angle so that the lateral aspect of the right leg is supported
Lateral thigh (LT)	1. Draw a horizontal line on the lateral side of the thigh at the height of the gluteal fold. 2. Mark the site at the midpoint of the sagittal thigh diameter.	Lying in a rotated position Participant rolls onto the left side with both knees at a 90° angle, with the right leg over the left leg

As seen in Table II, all the sites above are marked on the right side of body. Participant must be looking forward at all the times while marking the sites as the head movement will affect the accuracy. Moreover, all the ultrasound measurements require that the participant lying in a supine, prone, or rotated position [8]. Fig.14. shows all the marked sites on the right side of the body.

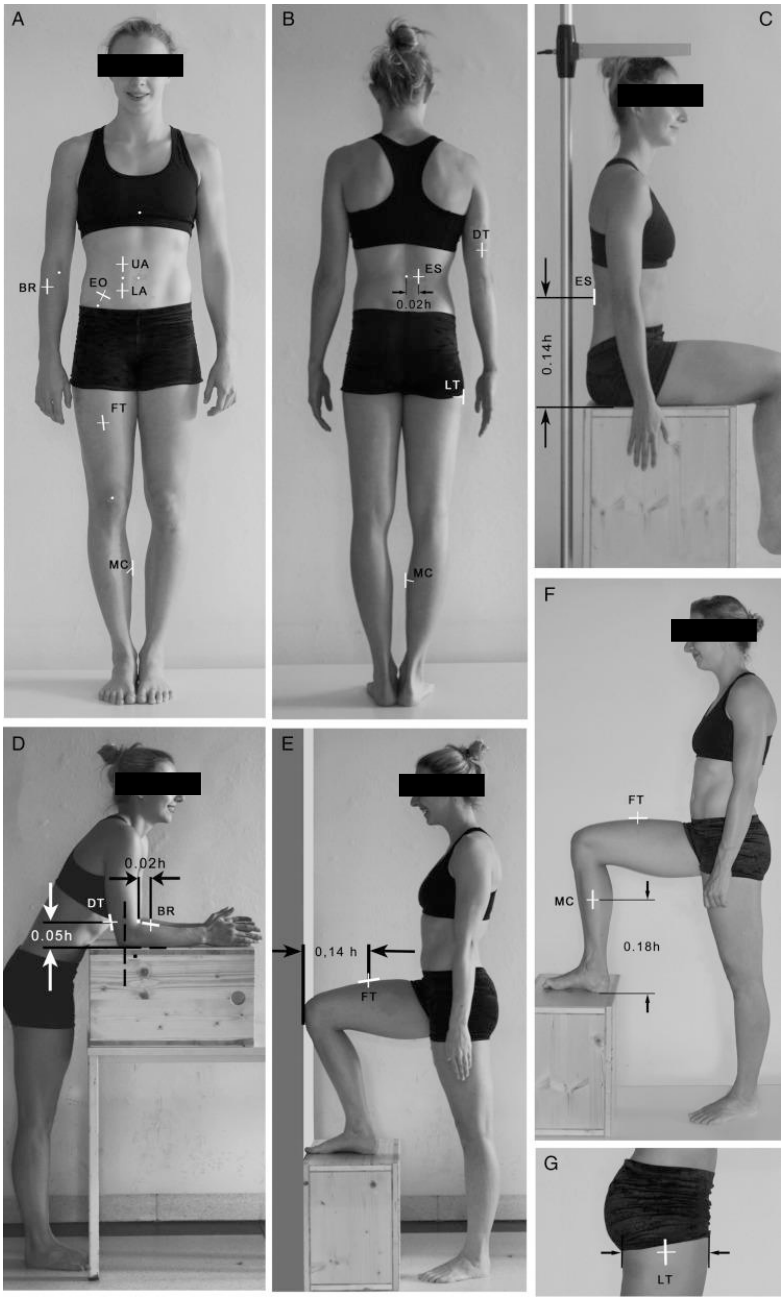

Fig. 14. Body positions when marking ultrasound sites. [8]

In illustration above (Fig.14.), h means the body height and all distances described, are in the percentage of body height. For instance, d= 0.02h means 2% of the body height.

3.2. Experiment 1.: Fat measurement with skinfold callipers

3.2.1 Setup

Before taking the measurements, the subject should be instructed that there might be slight discomfort as the calliper heads pinch the skin. During the skinfold measurements the subject should always be relaxed, this aids in manipulation of the skinfolds. All the readings are taken on the right side of the body, unless otherwise specified. The measurer raises the folds at the designated sites with index finger and thumb of the left hand and place the calliper 1 cm below the mark with the reading scale facing upwards [20]. The jaws of the calipers are applied at the right angles to the skinfold. Afterwards, the jaw pressure is released slowly, and measurement is taken 2-4 seconds after the calliper is settled. Fig.15. illustrates the pictorial form of the above information.

(a) (b)

Fig. 15. Calipers position while measuring skinfold thickness [20].

The settling of the calliper is particularly important as subcutaneous tissue is compressible, and any variation in the length of time will result in errors. Readings are then done to the nearest 1mm. For accuracy, three readings are taken at each skinfold and then averaged. Once the recordings are done, the skinfold is released, and the callipers are cleaned for future use [3].

3.2.2 Data Collection

For data collection, two subjects (1 male and 1 female) with different height and weight were chosen. The height was recorded to the closest centimeter (cm) and weight was recorded to the closest gram (g). Afterwards, the readings with the skinfold calipers were recorded at the sites given in Table II to the closest millimeter (mm). The full body readings were repeated thrice to get the average value at the sites. Table III shows, the data for both male and female subject.

TABLE III
RECORDED SAT THICKNESS VALUES FOR TWO SUBJECTS WITH SKINFOLD CALIPERS

	Measured Site	Reading 1 (mm)	Reading 2 (mm)	Reading 3 (mm)	Mean (mm)	Median (mm)	Std. Dev. (mm)
Subject 1 (male) Age: 23yrs Height: 176cm	Upper Abdomen (**UA**)	22	20	20	20.67	20	1.15
	Lower Abdomen (**LA**)	19	23	20	20.67	20	2.08
	Erector Spinae (**ES**)	14	15	15	14.67	15	0.58
	Distal Triceps (**DT**)	6	6	6	6.00	6	0.00
	Brachioradialis (**BR**)	3	3	4	3.33	3	0.58
	Front Thigh (**FT**)	13	13	14	13.33	13	0.58
	Medial Calf (**MC**)	9	9	9	9.00	9	0.00
	Lateral Thigh (**LT**)	16	17	17	16.67	17	0.58
Subject 2 (female) Age: 20yrs Height: 157cm	Upper Abdomen (**UA**)	27	26	23	25.33	26	2.08
	Lower Abdomen (**LA**)	30	27	27	28.00	27	1.73
	Erector Spinae (**ES**)	23	24	24	23.67	24	0.58
	Distal Triceps (**DT**)	12	13	13	12.67	13	0.58
	Brachioradialis (**BR**)	7	9	9	8.33	9	1.15
	Front Thigh (**FT**)	23	24	24	23.67	24	0.58
	Medial Calf (**MC**)	17	17	14	16.00	17	1.73
	Lateral Thigh (**LT**)	30	28	28	28.67	28	1.15

3.3. Experiment 2.: Fat measurement with Ultrasound

3.3.1 Setup

The setup for the ultrasound starts by placing gel on the head of the transducer and/or the skin at the measuring site. The gel helps in reducing artifacts and makes it easy to move the transducer along the skin by creating a strong bond. To avoid errors, a 5mm layer of ultrasound gel while measuring fat because of the compressibility of adipose tissue without any pressure on the transducer (ultrasound probe) [19]. With ultrasound turned on, the speed of sound is set to 1450m/s (for fat) rather than using the conventional speed of 1540m/s. If this parameter is not set correctly, the measurement error will be up by 6% and a small deviation of only 15m/s will generate a thickness measurement error of 1%.

After setting up parameters, the transducer is slid across the measuring site with a movement of ±5mm without any loss of contact with the skin [2]. A single scan will take only a few seconds and once completed, the image can be saved for analysis. Fig.16. illustrates the measurement sequence.

(a) (b)

Fig. 16. Measurement Sequence for an ultrasound image of the thigh [2]

Although scanning process is simple, the interpretation can be difficult. First, fascia between the superficial and depth subcutaneous adipose tissue (SAT) could be incorrectly identified as the boundary layer between subcutaneous fat and muscle. Second, applying pressure on the transducer can reduce the SAT layer by 25-37% depending on the measuring site [2]. There are some recommendations to overcome this issue but still a standard is required for other aspects of ultrasound measurement.

3.3.2 Data Collection

The data was collected using ultrasound machine with a 5MHz frequency linear transducer with the same subjects. The images were recorded over the course of three weeks with different sets of image properties to select the one with best definitions at the skin-fat and fat-muscle interfaces. The final set of images (in third week) were taken in a dark room to avoid some noise seen in the earlier images. Fig.17. shows a difference between the image quality taken during the first week and the third week.

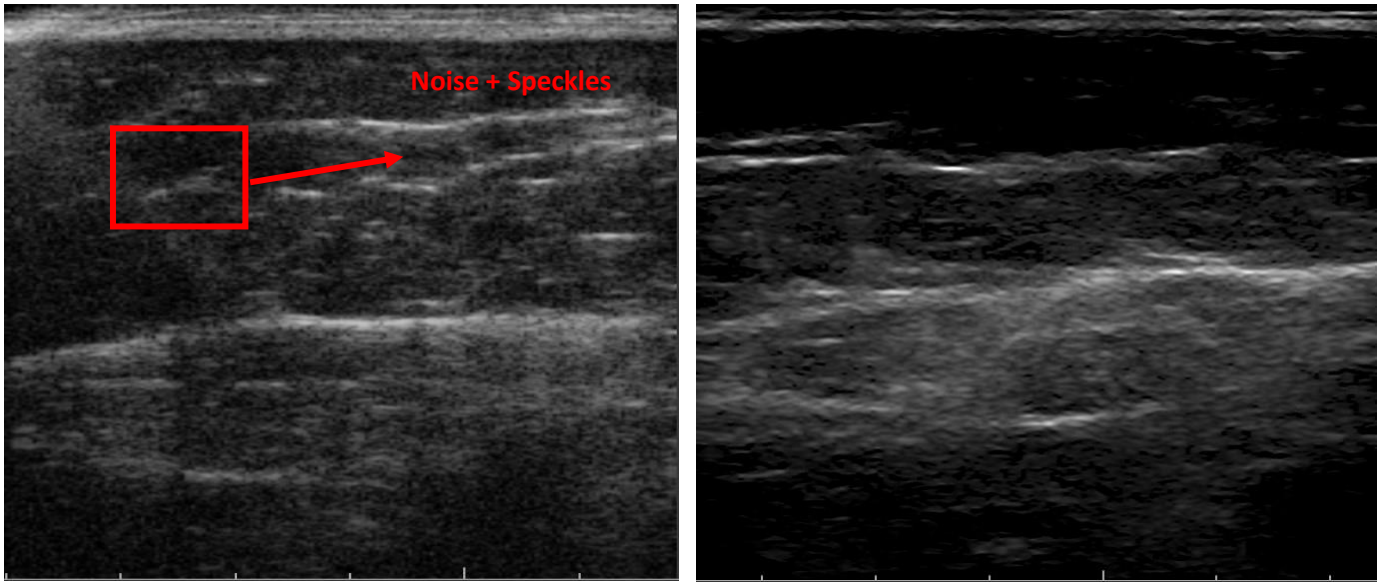

First week without adjustments (a)

Third week with the final adjustments (b)

Fig. 17. Comparison between first- and third-week results

As seen above in Fig.17., removal of noise and speckles using in-built software filters and by controlling the external factors, gives a promising idea about the thickness of SAT layer in the image by increasing the brightness across the edge where material interfaces changes.

The images below in Fig.18. are from the Subject 1 (male) taken in the third week of the data collection phase. The sites for these images are the same described in Table II.

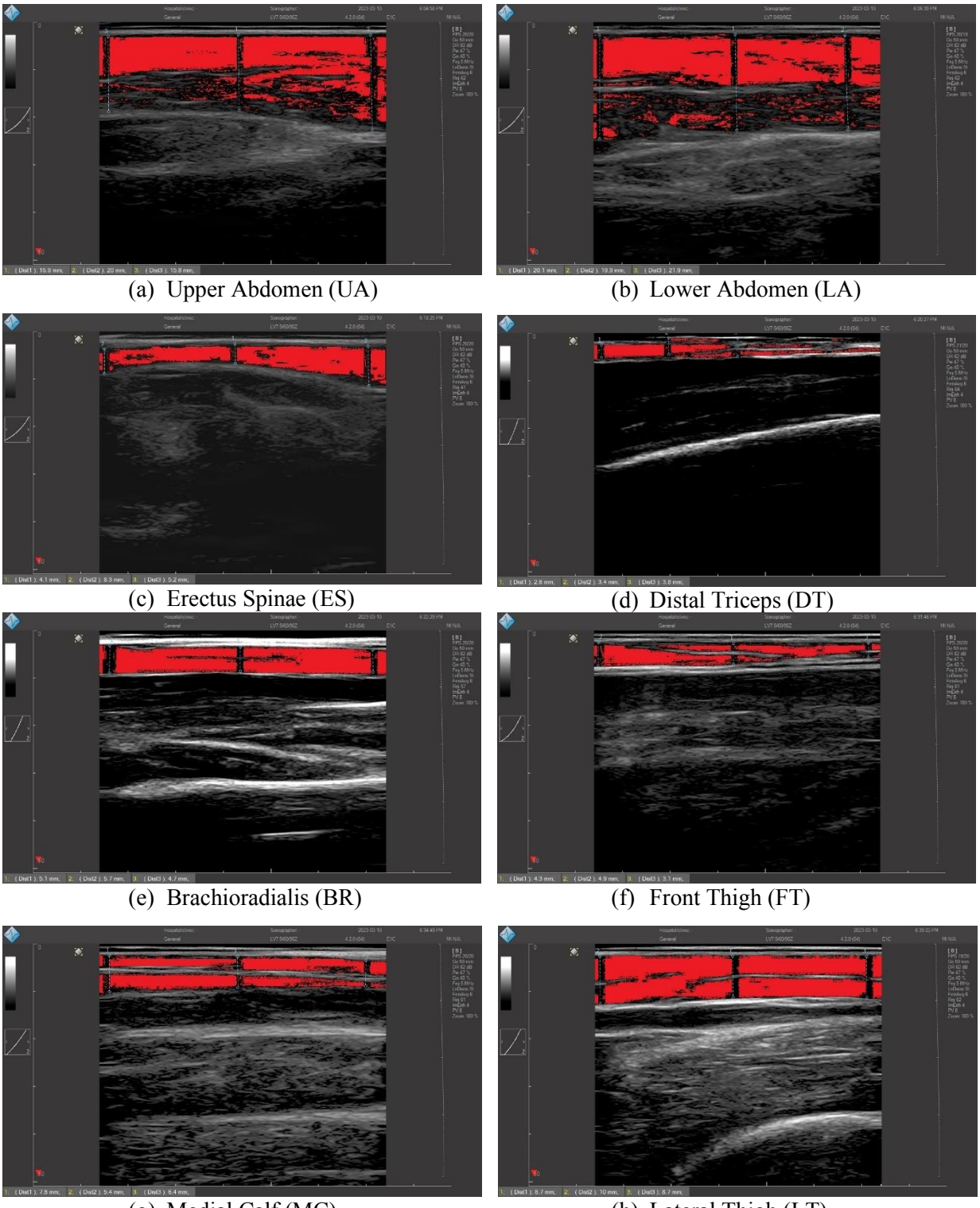

(a) Upper Abdomen (UA)
(b) Lower Abdomen (LA)
(c) Erectus Spinae (ES)
(d) Distal Triceps (DT)
(e) Brachioradialis (BR)
(f) Front Thigh (FT)
(g) Medial Calf (MC)
(h) Lateral Thigh (LT)

Fig. 18. Ultrasound Results for Subject 1 (Male). Red shows the observed SAT.

The next set of images in Fig.19. below belongs to Subject 2 (female). The readings are taken on the same day as Subject 1. and under the same external conditions.

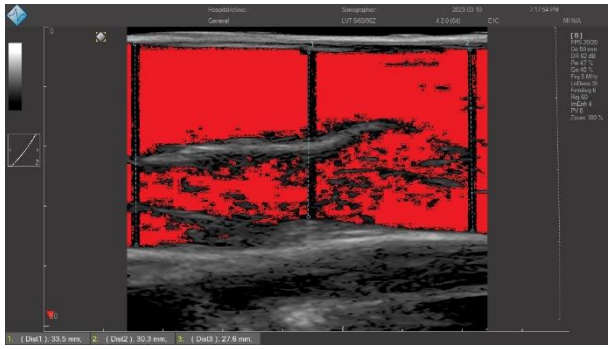

(a) Upper Abdomen (UA)

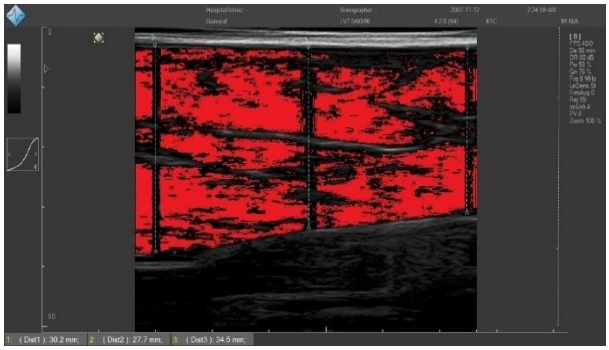

(b) Lower Abdomen (LA)

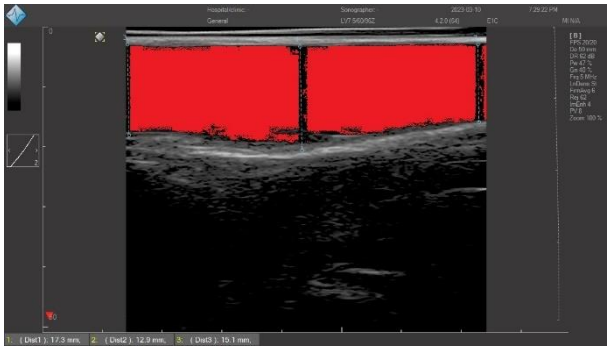

(c) Erectus Spinae (ES)

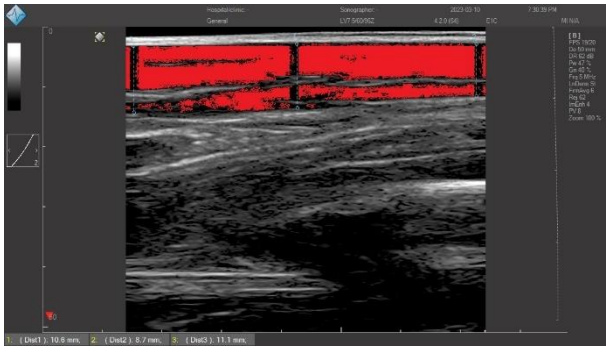

(d) Distal Triceps (DT)

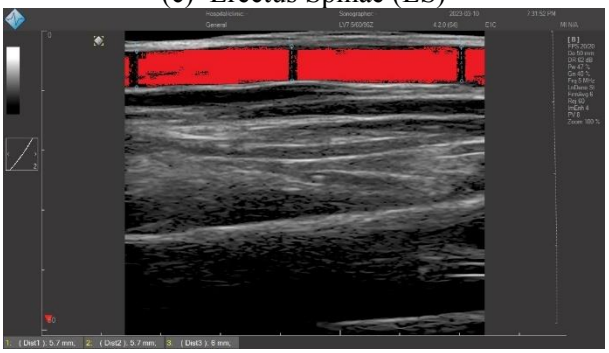

(e) Brachioradialis (BR)

(f) Front Thigh (FT)

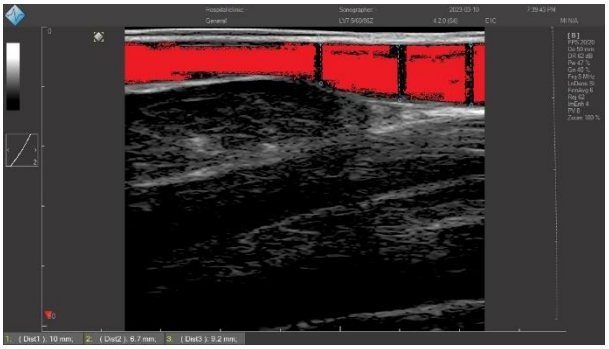

(g) Medial Calf (MC)

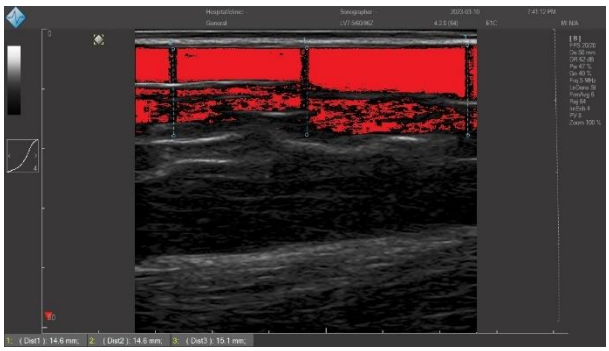

(h) Lateral Thigh (LT)

Fig. 19. Ultrasound Results for Subject 2 (Female). Red shows the observed SAT.

The above images were checked and approved by Kinesiology department's professors and researches at Simon Fraser University. The red sections in the above sets of images describe the thickness of Subcutaneous Adipose Tissue layer. Bearing that in mind, the red portion is not continuous which is due to the presence of connective tissues and embedded fibrous structures shown in Fig.2. The thickness of SAT layer in these images is measured by putting the markers on skin-fat interface (below dermis) and muscle-fat interface (above muscle fascia) using EchoWave software for the Ultrasound machine. Three sets of markers have been placed to measure thickness at three separate places and then the mean is taken to define the true SAT layer. The thickness has been measured to the nearest 0.1mm. Table IV below, provide the thickness readings from the images sets in Fig.18. and Fig.19. This Table, along with the Table III is further used to perform statistical analysis that helps making correlation between both the measuring methods.

TABLE IV
RECORDED SAT THICKNESS VALUES FOR TWO SUBJECTS WITH ULTRASOUND IMAGING

	Measured Site	Reading 1 (mm)	Reading 2 (mm)	Reading 3 (mm)	Mean (mm)	Median (mm)	Std. Dev. (mm)
Subject 1 (male) Age: 23yrs Height: 176cm	Upper Abdomen (**UA**)	15.9	20	15.8	17.23	15.9	2.40
	Lower Abdomen (**LA**)	20.1	19.9	21.9	20.63	20.1	1.10
	Erector Spinae (**ES**)	4.1	8.3	5.2	5.87	5.2	2.18
	Distal Triceps (**DT**)	2.6	3.4	3.8	3.27	3.4	0.61
	Brachioradialis (**BR**)	5.1	5.7	4.7	5.17	5.1	0.50
	Front Thigh (**FT**)	4.3	4.9	3.1	4.10	4.3	0.92
	Medial Calf (**MC**)	7.6	5.4	6.4	6.47	6.4	1.10
	Lateral Thigh (**LT**)	8.7	10.0	8.7	9.13	8.7	0.75
Subject 2 (female) Age: 20yrs Height: 157cm	Upper Abdomen (**UA**)	33.5	30.3	27.6	30.47	30.3	2.95
	Lower Abdomen (**LA**)	30.2	27.7	34.5	30.80	30.2	3.44
	Erector Spinae (**ES**)	17.3	12.9	15.1	15.10	15.1	2.20
	Distal Triceps (**DT**)	10.6	8.7	11.1	10.13	10.6	1.27
	Brachioradialis (**BR**)	5.7	5.7	6.0	5.80	5.7	0.17
	Front Thigh (**FT**)	15.4	16.5	14.5	15.47	15.4	1.00
	Medial Calf (**MC**)	10.0	6.7	9.2	8.63	9.2	1.72
	Lateral Thigh (**LT**)	14.6	14.6	15.1	14.77	14.6	0.29

Chapter 4. Results and Discussion

4.1. Results

4.1.1. Box Plot Comparison

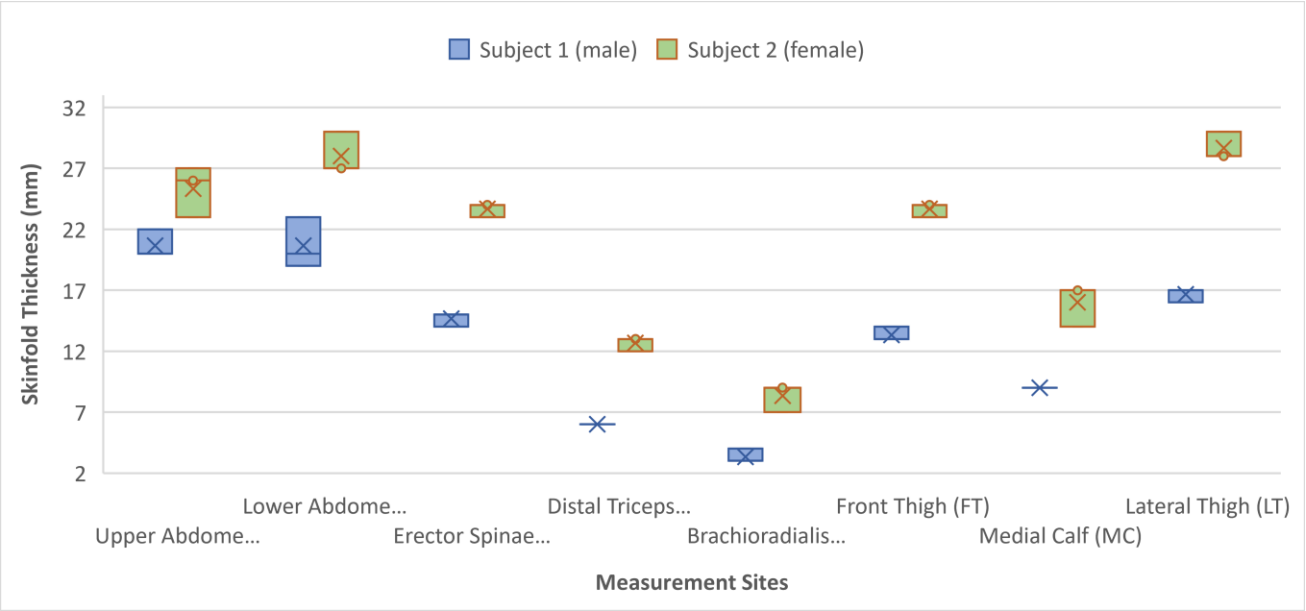

Fig. 21. Box plot for skinfold calipers data for both the subjects

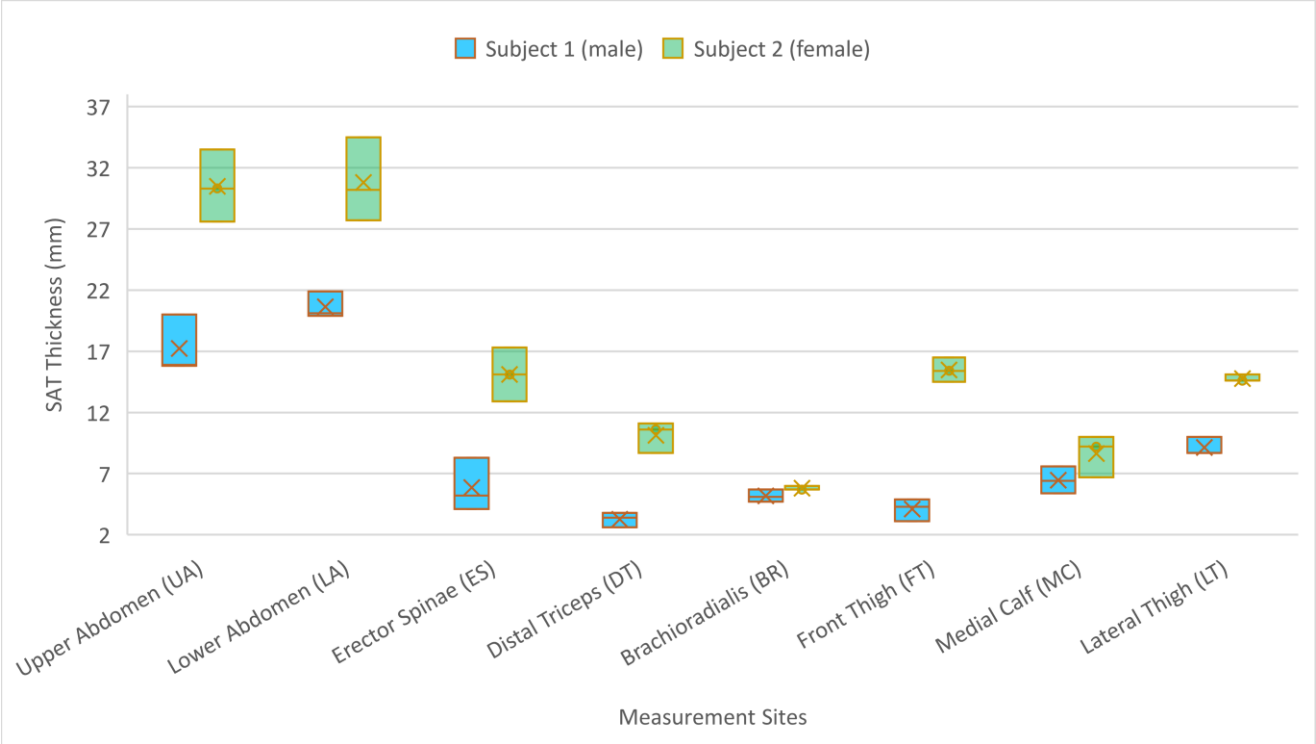

Fig. 20. Box plot for ultrasound imaging data for both the subjects

The data from Table III in experiment 1 is plotted to perform the box plot comparison between two subjects (male and female). Fig.20. shows the box plot for skinfold thickness using calipers describing the difference between body composition of subject 1 and subject 2. This comparison would be the base for our assumption about the data using ultrasound imaging.

Based on the above Fig.20., we can see that the distribution of skinfold thickness for both the subjects is quite different. The median skinfold thickness of subject 1 is lower than subject 2 for all the measuring sites. In addition, we observed smaller variability in measurements for subject 1 which is depicted by smaller box sizes and shorter whiskers. This is not the case for subject 2. These findings suggest that there may be differences in body composition for both the subjects since subject 1 is skinner than subject 2 and findings hold true for their body fat levels.

The generated comparison in Fig.20. should be replicated for the data collected by ultrasound imaging. In surface anthropometry using skinfold calipers, we not only measure the fat thickness but also take skin thickness into consideration as well which creates a significant difference in SAT thickness when done by Ultrasound Scanner. One more assumption is that the thickness of the bins in the box plot must be smaller in most cases as the fat is distributed formally between skin and muscles.

Keeping above assumptions in mind, the data collected by ultrasound scanner in Table IV is plotted in Fig.21. in the form of box plot for both subjects. We can see that the data from the ultrasound imaging follows the same exact trend as the data from using the skinfold calipers. Moreover, our assumption about the smaller bins is also true except in the abdomen region. This is because the fat in the abdomen covers the abdomen cavity which is a not plane as compared to the surface of a muscle. This is clearly shown by the measurements taken using ultrasound scanner.

Other factors that are significant here for explaining the thickness of bins in Fig.20. and Fig.21. are the setup for recording the measurements and precision by which it is recorded. In the case of skinfold calipers, the measurer grips the skinfold by hand and then take the measurement to the closest millimeter (mm) which varies very little, that is the reason why some bins in Fig.20. have zero width since all the measurements taken were exactly same. However, in the case of Ultrasound Imaging, the measurements were recorded to the closest 0.1 mm and the markers were applied over the entire image, not just over a part of the image.

4.1.2. Bland-Altman Analysis

Table V summaries the results and descriptive statistics for all the sites recorded using ultrasound imaging (USI) and the skinfold caliper (SC).

TABLE V
SUMMARIZED DATA FOR BOTH THE METHODS WITH RECORED TECHNICAL ERROR

	Measured Site	Method	Avg. Value (mm)	Difference (mm)	Median (mm)	Std Dev (mm)	rTEM (%)
Subject 1 (male)	UA	SC	20.67	3.44	20.00	1.15	4.56
		USI	17.23		15.90	2.40	11.35
	LA	SC	20.67	0.04	20.00	2.08	8.22
		USI	20.63		20.10	1.10	4.36
	ES	SC	14.67	8.8	15.00	0.58	3.21
		USI	5.87		5.20	2.18	30.31
	DT	SC	6.00	2.73	6.00	0.00	0.00
		USI	3.27		3.40	0.61	15.27
	BR	SC	3.33	1.84	3.00	0.58	14.16
		USI	5.17		5.10	0.50	7.95
	FT	SC	13.00	8.9	13.00	0.58	3.54
		USI	4.10		4.30	0.92	18.25
	MC	SC	9.00	2.53	9.00	0.00	0.00
		USI	6.47		6.40	1.10	13.91
	LT	SC	16.67	7.97	17.00	0.58	2.83
		USI	8.70		8.70	0.75	6.71
Subject 2 (female)	UA	SC	25.33	5.14	26.00	2.08	6.71
		USI	30.47		30.30	2.95	7.92
	LA	SC	28.00	2.8	27.00	1.73	5.05
		USI	30.80		25.60	1.23	9.12
	ES	SC	23.67	8.57	24.00	0.58	1.99
		USI	15.10		15.10	2.20	11.90
	DT	SC	12.67	2.54	13.00	0.58	3.72
		USI	10.13		10.60	1.27	10.20
	BR	SC	8.33	2.53	9.00	1.15	11.32
		USI	5.80		5.70	0.17	2.44
	FT	SC	23.67	8.2	24.00	0.58	1.99
		USI	15.47		15.40	1.00	5.29
	MC	SC	16.00	7.37	17.00	1.73	8.84
		USI	8.63		9.20	1.72	16.28
	LT	SC	28.67	13.9	28.00	1.15	3.29
		USI	14.77		6.70	1.51	1.60

In Table V, relative technical error of measurement (rTEM) is also provided. This is used to compare the performance of the measuring method. A lower rTEM value shows greater reliability, while higher value shows greater variability and potential error in the measurement [21]. We observe that in most cases rTEM is under acceptable range (10%) for both the methods. However, at some sites, measurement with ultrasound scanner provided a larger value of rTEM as compared to skinfold calipers for the same site. This is because those sites (e.g., Distal Triceps (DT)) on the body have smaller levels of fat and since ultrasound is collected information to the closest 0.1mm, any small deviation in the measurement will result in large error. This provides another conclusion that skinfold calipers work well with people who have less amount of fat deposits as there would be less deviation in the measurement and generating repeated results without any variability.

It should be noted that the average value column and difference column from the Table V will be used to create the Bland-Altman (B&A) chart. The B&A plot evaluates an agreement between two quantitative measurements. They set up a way to quantify agreement between two measuring methods by constructing limits of agreements. These limits are calculated by using the mean and the standard deviation (s) of the differences between two measurements. B&A analysis recommended that 95% of the data points should lie within ±2s, or more precisely, lie between ±1.96s. However, to perform B&A analysis, normal distribution of the differences must be verified. This analysis can be done by performing Shapiro Wilk Test [22].

The Shapiro-Wilk test is used to check the normality and carries a null hypothesis that the data collected follows a normal distribution. In this case, the data collected will be the difference between the mean values of both the methods at each skinfold site for both subjects. This test generates a p-value and if that p-value is less than 5% then the hypothesis will be rejected, and the data collected is not generated from a normal distribution. In case of the difference data from Table V, we got p-value equals 0.663 i.e., 66.3% which does support a normal distribution. Hence, we can move forward and generate the B&A plot for our data. Fig.22., shows the plot generated for our data which include 16 data points (8 for each subject).

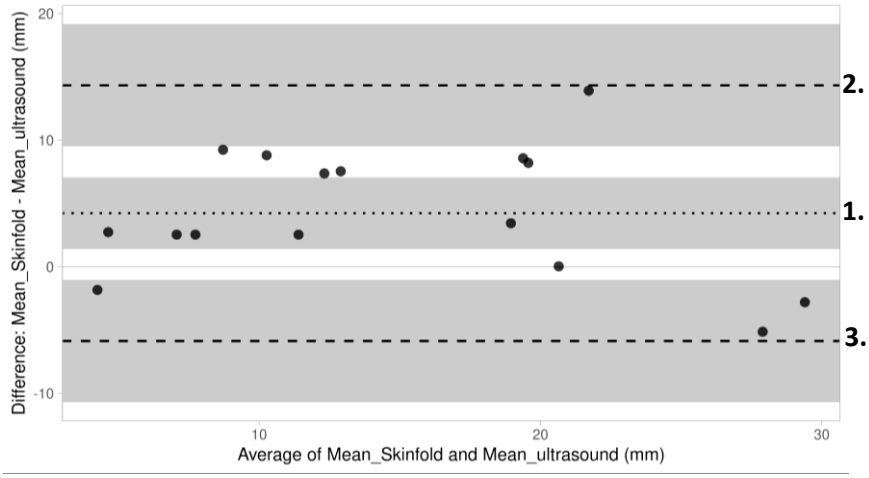

Fig. 22. Bland-Altmann plot for Mean-thickness values from ultrasound and skinfold calipers

The graph in figure above shows the data as scatter dots for both subjects. The dotted line (marked 1) indicates the average difference of 4.23mm and the dashed lines (marked 2 and 3) indicated the limits of agreement. The grey band reflects the 95% confidence intervals for each marked lines in the graph. The whole data is summarized below in the Table VI.

TABLE VI
RECORDED VALUES FROM THE BLAND-ALTMAN CHART

Parameter	Value	95%CI lower limit	95%CI upper limit
Mean difference	4.23	1.39	7.06
Upper Limit of Agreement	14.32	9.47	19.17
Lower Limit of Agreement	-5.87	-10.71	-1.02

4.1.3. Linear Regression

Linear regression analysis is used to predict the value of one variable based on the value of another variable. The method models a relationship between a response variable (dependent) and one predictor variable (independent), and the goal is to find the best fitting straight line that minimizes the discrepancies between the variables [23]. The equation for linear regression is represented as:

$$y = b_0 + b_1 x + \varepsilon \quad (4)$$

where y is the dependent variable, x is the independent variable, b_0 is the y-intercept and b_1 is the slope of the line. The error term is denoted by ε and is the part of the variable which cannot be explained by the model. In our case response variable is mean fat thickness using skinfold

calipers and mean fat thickness using ultrasound is our predictor variable. The graph from the linear regression model is in the Fig.23. with the line of best fit and estimated values according to that model.

The best fit line in the Fig.23. explains that the data of mean thickness from ultrasound can predict the mean thickness with skinfold calipers with a R^2 value of 0.6577. This means that 65.8% of the variation in the response variable around its mean. The R-value, which explains the correlation, is equals 0.811. This shows that there is a strong direct relationship between the mean thickness with ultrasound and the mean thickness with skinfold calipers.

The Fig.24. plots a prediction graph displaying regression line, 95% confidence interval, and 95% prediction interval. The prediction interval will tell us if a future observation is made, then in which interval it will fall according to the uncertainty levels recorded in the current data.

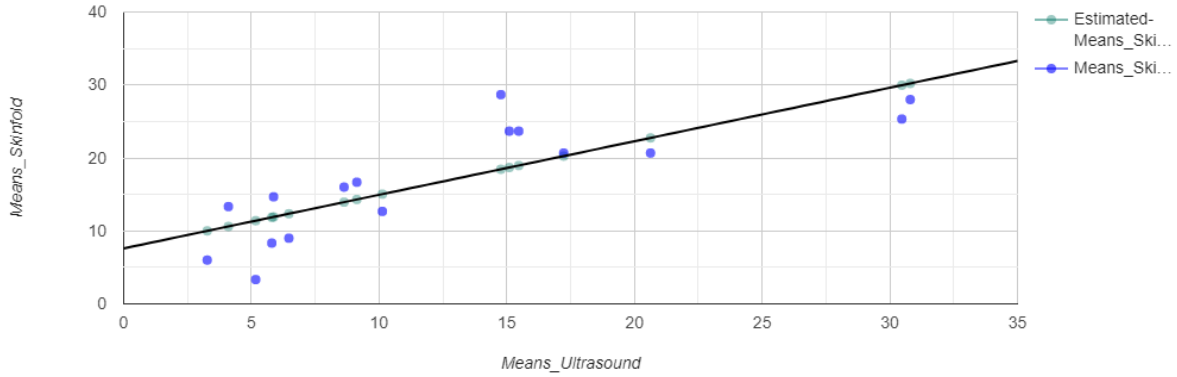

Fig. 23. The line of best fit for the data Mean-thickness values from skinfold calipers and ultrasound.

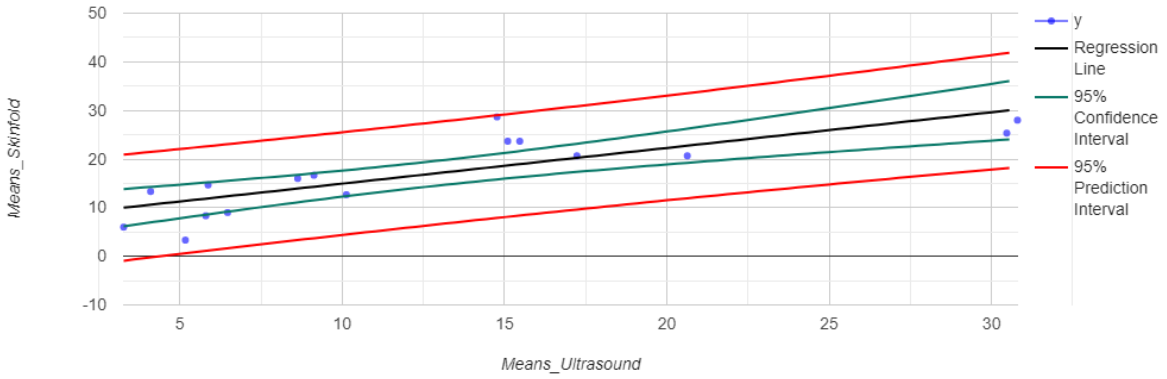

Fig. 24. Shows the regression line for the fitted data with 95% confidence interval and prediction interval.

From the Fig.24., we see that all the data points lie within the 95% prediction interval are there are no outliers in our data. Additionally, it was noticed that most data lie within the 95% confidence interval which means greater strength of our regression model. The equation of best fit line (regression line) is given by:

$$Y = 7.6032 + 0.734X \tag{5}$$

$$Mean_{Skinfolds} = 7.6032 + 0.734Mean_{Ultrasound} \tag{6}$$

Although we have the relationship between both methods, we do not know the extent by which this data will follow the expected values, also known as the goodness of a fit. A residual plot can be used to access this and Fig.25. shows a residual plot for the collected data.

The points in the graph of residuals are calculated using the regression model equation and actual values from the data. We can observe that the residuals are small except at two points which is close to +10 and -10 on the graph, respectively. The Shapiro-Wilk test on the residual datapoints give p-value equals 0.706. This shows that even the residual errors from the above regression model follow normal distribution.

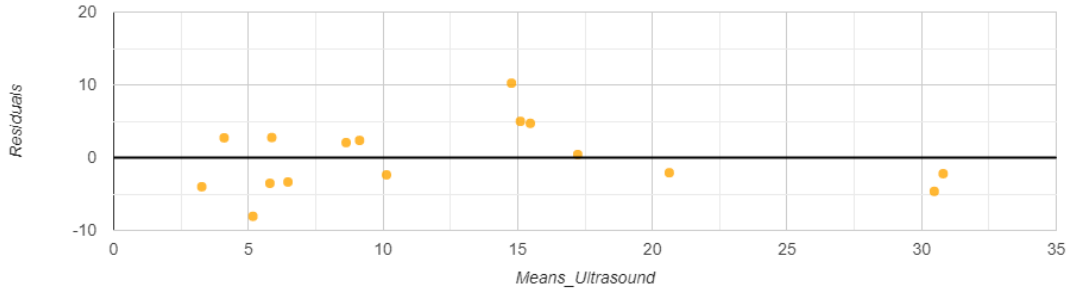

Fig. 25. Residual plot for skinfold calipers and ultrasound data

4.2. Discussion

The primary goal of this study is to analyze the comparison of adipose tissue thickness with ultrasound and skinfold calipers. Ultrasound allows measurement of SAT thickness in an uncompressed state and therefore eliminate any inaccuracies. From our study, the skinfold calipers appeared to overestimate SAT thickness compared with ultrasound imaging, especially at the regions with higher levels of fat deposits [24]. While using the calipers, the measurer holds the skinfold along with a double layer of skin, whereas ultrasound only needs to go through a single layer of skin [21]. The only exception where the result from ultrasound was higher than

the skinfold calipers was at the abdominal region (Fig.20. and Fig.21.). This is because ultrasound can detect both subcutaneous and visceral adipose tissue, the boundary between which is less noticeable. The observation made in our study concur with the results from other conducted studies.

The results of the regression analysis show a strong positive correlation (R=0.811) between mean skinfold thickness measured by calipers and ultrasound imaging, explaining 65.6% of the variation in the response variable around its mean. However, a strong correlation does not necessarily imply that the two methods are in agreement. It is also important to consider the limits of agreement (LOA) from the Bland-Altman chart, as wider LOA lines suggest greater disagreement between the methods [10]. Noticed in Fig.22., the LOA lines are wide since the methods used are not measuring the same thickness in the same technique. Nevertheless, every data point lies within the LOA, suggesting that the calipers and ultrasound are in good agreement on average, but caution should be taken when interpreting individual measurements.

Overall, the findings suggest that ultrasound may be a reliable method for measuring subcutaneous adipose tissue thickness, particularly in situations where caliper measurements may be difficult or impractical to obtain. It is also important to recognize that there may be some degree of measurement error associated with either method, and that the accuracy of the measurements may be influenced by factors such as operator's ability, measurement site, and patient characteristics [25]. Therefore, it is recommended that observers must take part in structured training programs that consist of site-marking, managing the ultrasound system, and guided exercises and interobserver comparison.

Skinfold calipers being readily available and widely used in clinics, have several limitations compared to ultrasound systems. For example, skinfold calipers may overestimate subcutaneous fat, leading to incorrect calculation of body fat and potential misinterpretation of results. Additionally, the hydration status of the subject at the time of assessment can affect results, and applying the calipers to harder skin can cause discomfort for the subject. The end range of the calipers (roughly 60mm) can also limit their use for certain populations and lead to potential embarrassment for athletes among their peers or clinicians [10]. Furthermore, calipers may be impractical or impossible to use on individuals with spinal cord injury or reduced mobility.

Despite being unpopular, ultrasound managed to tackle the limitations of skinfold calipers and supplied a better method that can be used for any clinical population. Being non-invasive and non-radiative, the method is less affected by the skin thickness and hydration levels of the subject. As investigated above in results, ultrasound manages to provide SAT thickness more precisely due to its ability of showing the boundaries of adipose tissue layer [2]. Additionally, ultrasound is not limited by the end range of skinfold calipers and can be used on any body part, including the abdominal area, which is not accessible by calipers. However, like every other method it has its own limitations. The advantages and disadvantages of ultrasound for assessing body fat are summarized below in table VII [2].

TABLE VII
ADVANTAGES AND LIMITATIONS OF ULTRASOUND AS FAT MEASURING DEVICE

Advantages	Limitations
Lower cost than laboratory methods	Higher cost than field methods
High accuracy and precision in the hands of an experienced technician	Requires experienced technician with considerable skills
Capable of regional and segmental measurements	Measurement procedures and techniques are not yet standardized
Minimal tissue compression	Inherent artifacts (fascia, etc.)
Non-invasive and no ionizing radiation	
Applicable for testing in the field	
Can measure other tissue thicknesses (muscle and bone)	
Short testing time, rapid procedure	

Chapter 5. Conclusion and Future Work

5.1 Conclusion

To summarize, despite being available for over 50 years, ultrasound still is an underutilized technology for body composition assessment. Nonetheless, this study shows that ultrasound is a fast, accessible, and cost-effective method with good accuracy and reproducibility. The results showed that ultrasound is highly correlated with skinfold calipers, but with some variability between the two for a few measuring sites. Despite that, ultrasound stays advantageous over calipers due to its ability to measure fat thickness at any body site, assess regional composition, and lack of range limit. Moreover, ultrasound has the added advantage of being able to provide unique assessments for specific clinical populations, which is not possible with skinfold calipers. However, the lack of standardized procedures and operator dependency are limitations to its use as a body composition technique. The technology has the potential to become even more widely used with the development of portable and affordable ultrasound devices. Therefore, it is recommended that standardized procedures must be developed and adopted for the use of ultrasound in body composition assessment to maximize its potential and ensure its accuracy and reliability.

5.2 Future Work

While this study managed to accomplish the set objectives and made significant contributions to the topic, there are still several areas for future study that could build upon the findings of this thesis research. Some promising directions for future work include:

- One important aspect for the future would be eliminating the thickness of fibrous structures from the fat layer to find the true thickness of SAT. Those fibrous structures can affect the reading by atleast 1-2mm depending on the skinfold location. This can be done by using image segmentation and masking the relevant areas only. Additionally, rather than using three markers within the region of interest, an algorithm can be designed that will generate 200-300 thickness values and take the mean for true thickness.

- Another promising area to investigate is the equation for calculating total body fat percentage based on the marked skinfold locations shown in Table II. There are various equations for calculating body fat percentage that are being used successfully for a long time. These include equations given by Jackson-Pollock, Durnin and Womersley, Yuhasz, Peterson and more. However, all these equations are for skinfold calipers and are either focused toward one geographical population or have different number of skinfolds measuring sites. Therefore, a set of equations for ultrasound scanner are needed with a set number of measuring sites. This can be done on a larger scale by first doing MRI scans of subjects for calculating the true body composition and then creating a multiple regression model based on results from MRI scans and SAT thickness from ultrasound. The regression model with maximum value of R^2 (acceptable above 90%) will give us the model equation that can be used with ultrasound scanner.

- To explore the direct effects of the selection of measuring sites on total body fat calculation, future work can include the Principal Component Analysis (PCA) of these sites. PCA is a dimensionality reduction method, often used in large datasets by transforming a large set of variables into smaller ones while retaining the maximum information they possess. In the case of this study, the datasets can be the data from the multiple measuring sites including the one from Table V and new added ones. By running this analysis, we can depict which skinfold sites contribute most to the total body fat mass calculation and drop the redundant ones.

Other than the above listed, there are more research possibilities, and the findings from this study creates a solid foundation for further exploration. The continuation on the any of the above mentioned will deepen our understanding of the topic and help in presenting significant contributions to the related field.

References

[1] M. P. McRae, "Male and female differences in variability with estimating body fat composition using skinfold calipers," *J Chiropr Med,* vol. 9, no. 4, 2010.

[2] D. Wagner, "Ultrasound as a tool to assess body fat.," *Journal of obesity,* 2013.

[3] P. S. K. d. R. J. Hume, "Non-imaging Method: Surface Anthropometry.," in *Best Practice Protocols for Physique Assessment in Sport.* , Singapore, Springer, 2018.

[4] T. M. W. Ackland, "Imaging Method: Ultrasound," in *Best Practice Protocols for Physique Assessment in Sport.* , Singapore, Springer, 2018.

[5] F. Esparza-Ros, A. C. Moreira, R. Vaquero-Cristobal and C. Barrigas, "Differences between Four Skinfold Calipers in the Assessment of Adipose Tissue," *Nutrients MDPI,* no. 10, 2022.

[6] J. L. Prince and J. M. Links, Medical Imaging Signals and Systems, Upper Saddle River: Pearson, 2015.

[7] A. Kelso, K. Vogel and J. Steinacker, "Ultrasound measurements of subcutaneous adipose tissue thickness show sexual dimorphism in children of three to five years of age," *Acta paediatrica (Oslo, Norway : 1992),* p. 514–521, 2019.

[8] W. Muller, T. Lohman, A. Stewart, R. Maughan, N. Meyer, L. Sardinha, N. Kirihennedige, A. Regaunt-Closa, V. Risoul-Salas, J. Sundgot-Borgen, H. Ahammer, F. Anderhuber, A. Furhapter-Rieger, P. Kainz, W. Materna, U. Pilsl, W. Pirstinger and T. Acland, "Subcutaneous fat patterning in athletes: selection of appropriate sites and standardisation of a novel ultrasound measurement technique: ad hoc working group on body composition, health and performance, under the auspices of the IOC Medical Commission," *British journal of sports medicine,* vol. 1, no. 50, pp. 45-54, 2016.

[9] A. E. Smith-Ryan, M. N. Blue, E. T. Trexler and K. R. Hirsch, "Utility of ultrasound for body fat assessment: validity and reliability compared to a multi-compartment criterion," *HHS Public access,* 2016.

[10] N. Selkow, B. Pietrosimone and S. Saliba, "Subcutaneous thigh fat assessment: a comparison of skinfold calipers and ultrasound imaging.," *J Athl Train,* vol. 1, no. 44, pp. 50-54, January-February 2011.

[11] J. Hoffmann, J. Thiele, S. Kwast, M. A. Borger, T. Schroter, R. Falz and M. Busse, "Measurement of subcutaneous fat tissue: reliability and comparison of caliper and ultrasound via systematic body mapping," *Scientific Reports,* 2022.

[12] W. R. Hedrick, Ultrasound physics and instrumentation, St. Louis: Mosby, 1995.

[13] N. M. Tole, BASIC PHYSICS OF ULTRASONOGRAPHIC IMAGING, Malta: World Health Organization, 2005.

[14] "BASIC PHYSICAL PRINCIPLES OF ULTRASOUND," 2012.

[15] J. Y. Chi Ng, *Automatic Measurement of Human Subcutaneous Fat,* Vancouver: University of British Columbia, 2006.

[16] M. Postema, S. Kotopoulis and K.-V. Jenderka, "Physical principles of medical ultrasound," 2019.

[17] S. P. Grogan and C. A. Mount, "Ultrasound Physics and Instrumentation," *StatPearls,* 2022.

[18] S. Ananthi, "Ultrasound Medical Diagnostic Instrumentation," in *Textbook of Medical Instruments*, New Age International Ltd, 2006, pp. 253-258.

[19] F. Ponti, A. Cinque, N. Fazio, A. Napoli, G. Gugliemi and A. Bazzocchi, "Ultrasound imaging, a stethoscope for body composition assessment.," *Quantitative imaging in medicine and surgery,* vol. 8, no. 10, p. 1699–1722, 2020.

[20] "How to Measure Body Fat Percentage Using Skinfold Calipers," Registered Nurse RN, [Online]. Available: https://www.registerednursern.com/measure-body-fat-percentage/. [Accessed 25 March 2023].

[21] Z. Lewandowski, E. Dychała, A. Pisula-Lewandowska and D. Danel, "Comparison of Skinfold Thickness Measured by Caliper and Ultrasound Scanner in Normative Weight Women," *Int. J. Environ. Res.Public Health,* no. 19, 2022.

[22] D. Giavarina, "Understanding Bland Altman analysis," *Biochemia Medica,* vol. II, no. 25, pp. 141-151, 2015.

[23] J. Pineau, J. Filliard and M. Bocquet, "Ultrasound techniques applied to body fat measurement in male and female athletes.," *Journal of athletic training,* vol. 2, no. 44, p. 142–147, 2009.

[24] A. Ingle, N. Kashyap, S. Trivedi, R. Choudary, G. Suryavanshi, P. Thangaraju and K. Bagale, "Assessment of Body Fat Percentage Using B-Mode Ultrasound Technique versus Skinfold Caliper in Obese Healthy Volunteers," *Cureus,* vol. 3, no. 14, 2022.

[25] H. M. F.-R. A. Müller W, "Body composition in sport: a comparison of a novel ultrasound imaging technique to measure subcutaneous fat tissue compared with skinfold measurement," *British Journal of Sports Medicine,* no. 47, pp. 1028-1035, 2013.

[26] J. Wilbur, "Imaging Ultrasound Hardware Basics," 24 November 2019. [Online]. Available: https://github.com/open-ultrasound/Specifications/blob/master/Hardware.md. [Accessed 11 April 2023].

Appendix-A

Important points for avoiding errors and for standardising the US technique:

- Besides setting the sound speed correctly, it is also important to set all US imaging parameters that decide the image quality adequately for a given anatomical structure. For example, using a too high gain, inadequate time-gain-compensation, inadequately positioned foci, or too low frequency, would broaden the borders and reduce image contrast. This would also decrease substantially the accuracy of tissue border detection.

- The marker on one side of the linear US probe (a linear probe is necessary for accuracy reasons) is always directed upwards (cranially) or upwards-and-to-the-left. This corresponds to the usual application of diagnostic US probes in medicine.

- Measurements are usually made on the right side of the participant's body. The middle of the probe is placed exactly above the landmarked site and held perpendicular to the skin. The investigator's hand may contact the participant's body to stabilise and guide of the probe, but there must be a minimum distance of 5 cm between the support hand and the probe. Otherwise, the pressure might distort the fat profile.

- Always use a thick layer of US gel (at least 3 to 5 mm, avoid any air bubbles) between the probe and the skin. In the image, a black band above the skin corresponds to this gel layer. This is vital for the assessment of the US image because it ensures that there is no pressure on the skin (which would compress the SAT layer). If the image quality is not good enough, it can be useful to restart the imaging with a new layer of gel on the probe. During US imaging, check that a dark band of about 3 to 5 mm above the skin can be seen on the screen.

- The light should be dimmed in the examination room and the general gain, and the depth gain compensation should be set such that the US image of the SAT is very dark and only the structures of interest can be seen clearly. Too much gain would result in displaying "noise" in addition to real objects and in a decrease of resolution.

- The borders of SAT should be clear to the investigator when capturing the US image. The SAT layer should appear dark in the US image (otherwise the gain is too high); eventually some light lines which correspond to fibrous structures can be seen embedded

in the fat. The investigator must make sure that the borders of the SAT (end of skin on the upper side and muscle fascia on the lower side of the SAT layer) are clearly visible as white bands without any interruption.

- In case of doubt about the location of the muscle fascia (i.e., the lower border of the SAT), compress the SAT with the US probe in order to distinguish between SAT and the muscle; this is essential in such cases to avoid erroneous image evaluation (misinterpretation of intermediate fasciae, like Camper's fascia in the abdomen). When borders are clear, start the imaging again with a new 5 mm layer of gel.

- Image evaluation should be done soon after having captured the US image. In case this is not possible, all US systems permit text to be inserted onto the US image. This feature can be used to mark the fascia of the muscle underneath the SAT (to prevent misinterpretations later). Of course, such annotations must be outside the region of interest.

- In case a vein appears in the US image (black band without any grey speckle), move the probe beside the vein. For example, at the brachioradialis (BR) site, the vena cephalica is sometimes in the field of view. This might erroneously lead to a measurement of the vein thickness instead of the SAT thickness.

Appendix-B

Ultrasound Device Circuitry

Transmitter Circuit

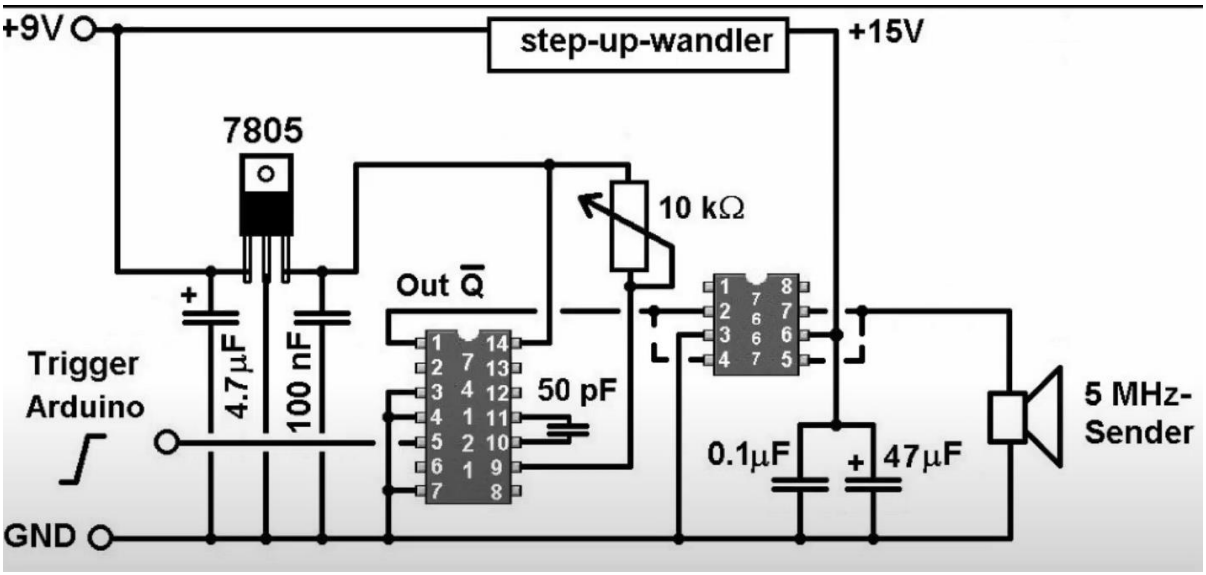

Receiver Circuit

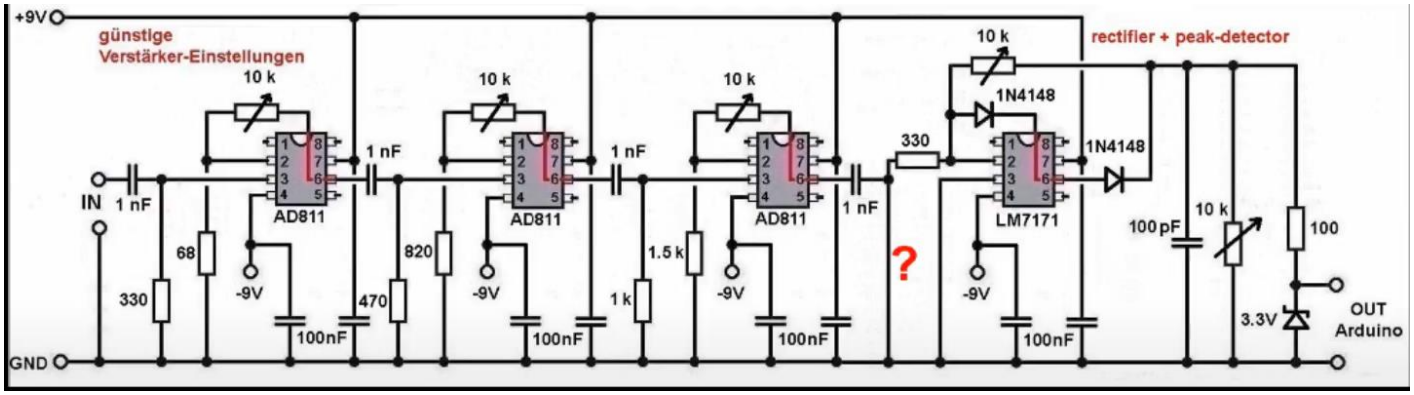

PCB Assembly